Coral Propagation: Land-based and Offshore Nursery Phase VII

Final Report

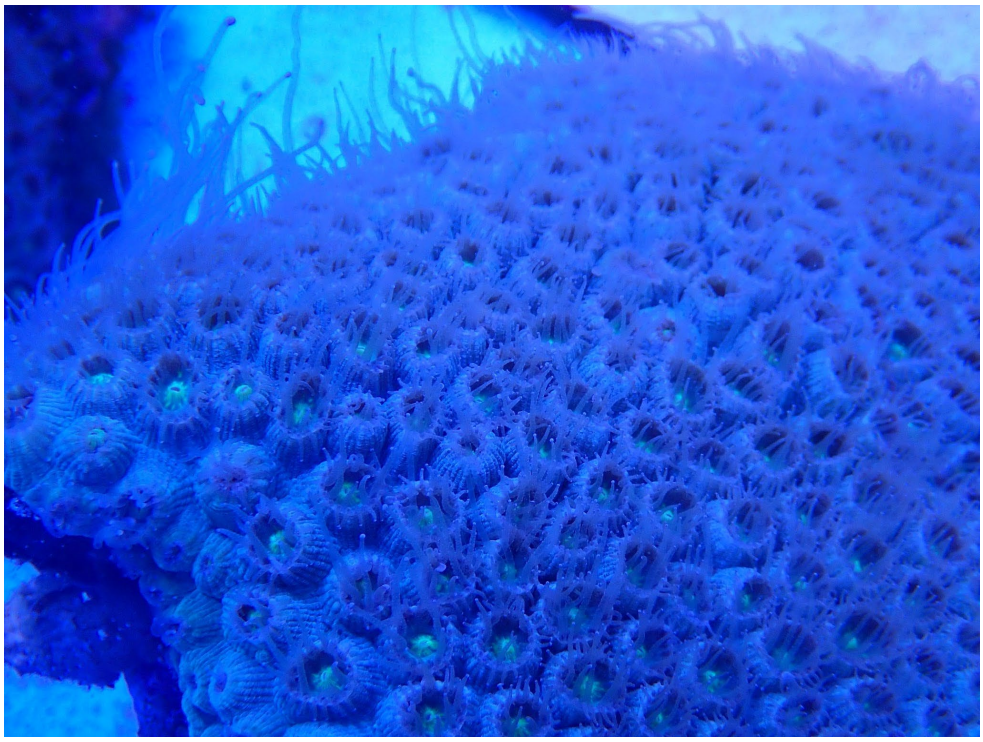

Coral Propagation: Land-based and Offshore Nursery Phase VII
Final Report

Prepared By:

Dr. Joana Figueiredo

Dr. David Gilliam

Dr. Peter Schupp

Dr. Ronen Liberman

Dr. Eloy Martinez

Dr. Matías Gómez-Corrales

Claire Denker

Morgan Hightshoe

Laura J. Fiegel

Nova Southeastern University

Halmos College of Arts and Sciences

8000 N. Ocean Drive

Dania Beach. FL 33004-3078

June 15, 2026

Completed in Fulfillment of Grant C5A9EC for

Florida Department of Environmental Protection

Coral Protection and Restoration Program

8000 N Ocean Dr.

Dania Beach, FL 33004

This report should be cited as follows:

Figueredo, J., Gilliam, D., Schupp, P., Liberman, R., Martinez, E., Gómez-Corrales, M., Denker, C., and Hightshoe, M., Fiegel, L., 2026. Coral Propagation: Land-based and Offshore Nursery (Phase VII). Final Report. Florida DEP. Dania Beach, FL.

This report was prepared for the Florida Department of Environmental Protection's (DEP) Coral Protection and Restoration Program by Nova Southeastern University. Funding was provided by the DEP Award No. C5A9EC. The statements, findings, conclusions, and recommendations are those of the author(s) and do not necessarily reflect the views of the State of Florida or the Florida Department of Environmental Protection.

Management Summary (300 words or less)

Nova Southeastern University's (NSU) *ex situ* and *in situ* coral nurseries, which maintain colonies of priority species, focused on scaling up capacity and long-term survival. The *ex situ* nursery cultured 132 broodstock colonies which safeguarded genotypes that originated from the Kristen Jacobs Coral Aquatic Preserve (KJCAP). The broodstock successfully underwent annual spawning in captivity. Tending to the adult colonies before and after spawning required heavy feeding and good water quality pre-spawning and the enactment of treatments for recovery post-spawning to ensure high reproductive output and long-term survival of captive corals. In total, 562 recruits from 2024 produced from six priority species (*Colpophyllia natans, Diploria labyrinthiformis, Orbicella faveolata, Montastraea cavernosa, Pseudodiploria clivosa, and Pseudodiploria strigosa*) were moved to NSU's offshore coral nursery for later grow-out. For coral recruits transferred to the offshore nursery, survival was generally high (100%) for four of the six species, with the others likely being limited by size and algal overgrowth. The use of large mesh predator exclusion devices (PED) was effective at eliminating the majority of predation. Direct outplant survival after three months was high (≥ 95%) for all species, likely due to the application of predator exclusion cages.

Executive Summary (max 1 page)

NSU's land-based nursery had three goals: 1) preserve the genetic diversity of five priority coral species and sexually propagate them to generate corals of high genetic diversity to restore Broward County's reefs within the KJCAP; 2) optimize the culture methodology of corals so that production is maximized while production cost, labor and time are minimized; and 3) train new individuals in coral restoration. Considerable progress has been made over the past six phases of the project, with success hinging on continued research to increase cost-efficiency of NSU's propagation pipeline and the skills of our staff.

In this phase, we utilized the Tri-Annual Coral Spawning Chamber (Tri-ACSC) to induce the staggered spawning of the corals within our biobank, i.e., have *M. cavernosa* and *O. faveolata* spawn in July/August, *P. clivosa* in January/February, *C. natans* and *P. strigosa* in April/May and

D. labyrinthiformis in May/June. This year the cycles imposed on the broodstock were abnormal, i.e. aside from *M. cavernosa* and *D. labyrinthiformis* which spawned as expected in the aquaria, the other species were exposed to a 16 or 19 month cycle, thus it is not surprising these did not spawn this year. We expect spawning will resume next year as corals will have completed a full 12 month cycle under the correct environmental cues. Additionally, we tested the efficiency of cycloprodigiosin (CYPRO) inducing settlement and metamorphosis on larvae of *D. labyrinthiformis* from the KJCAP, ran a genome-wide parentage analysis, and assessed the energetics of coral early life stages.

NSU's aquaria are outfitted with highly precise temperature and artificial lighting control systems to ensure the survival, growth and highly synchronized sexual reproduction of corals *ex situ*. The adult coral colonies held in NSU's recirculating aquaculture systems produced hundreds of thousands of larvae that were reared under optimized lab conditions at NSU or donated to other coral nurseries for rearing. Five hundred and sixty two corals from six priority species produced during the previous phase of this project (2024 spawning) were moved into NSU's offshore coral nursery for acclimation, while 160 recruits were directly outplanted to a Broward County reef site. *Diploria labyrinthiformis* larvae showed clear, source-specific metabolic differences, with field-derived larvae maintaining higher metabolic performance at warmer temperatures while nursery-derived larvae performed best near 26°C. These findings highlight the strong influence of parental thermal history on larval physiology and provide actionable guidance for optimizing nursery rearing conditions to improve larval survival and restoration outcomes.

Acknowledgements

Thank you to the Florida Fish and Wildlife Conservation Commission State Wildlife Grant Program and the Florida Department of Environmental Protection Office of Resilience and Coastal Protection for supporting these efforts. We thank the Florida Coral Disease Advisory Committee for the large number of volunteers assisting in the meeting and planning of coral disease efforts. A big thank you to the Miami-Dade County Department of Regulatory and Economic Resources

Environmental Resources Management Restoration & Enhancement Section for their help with field efforts. We thank Lisa Gregg for assisting with permitting. We thank NSU Oceanographic Center's staff, students, and volunteers for diving and lab assistance. Thank you to the DEP Coral Protection and Restoration staff including Kathleen Czaia and Conner Obsorn for contract and report review coordination.

Table of Contents

List of Acronyms

CBASS	Coral Bleaching Automated Stress System
CCA	Crustose Coralline Algae
CRRAM	Coral Reef Restoration and Monitoring Lab
CYPRO	Cycloprodigiosin
DAFM	Days After Full Moon
DEP	Department of Environmental Protection
FCR	Florida's Coral Reef
FSW	Filtered Seawater
FWC	Florida Fish and Wildlife Conservation Commission
GHOC	Guy Harvey Oceanographic Center
KJCAP	Kristen Jacobs Coral Aquatic Preserve
MAS	Minutes After Sunset
MeOH	Dissolved Methanol
MLER	Marine Larval Ecology and Recruitment Lab
NSU	Nova Southeastern University
PAR	Photosynthetically Active Radiation
PED	Predator Exclusion Device
POS	Positive Control
SAL	Special Activity License
SCTLD	Stoney Coral Tissue Loss Disease
SNP	Single Nucleotide Polymorphisms
TFA	The Florida Aquarium

Tri-ACSC	Tri-Annual Coral Spawning Chamber
UNCW	University of North Carolina Wilmington
WGS	Whole-Genome Sequencing

- **PROJECT DESCRIPTION**

The coral cover on Florida's Coral Reef (FCR) has been declining due to synergistic impacts of natural and anthropogenic derived disturbances such as multi-year disease outbreak events, heat stress, and hurricanes. Approximately 21 species of corals, including Endangered Species Act-listed and primary reef-building species, are highly susceptible to stony coral tissue loss disease (STCLD) which often results in whole colony mortality. In the northern region of Florida's Coral Reef, particularly the KJCAP, the abundance of corals has suffered a decline of over 30% (Walton et al. 2018). These catastrophic losses are changing the function and utilization of coral reefs. Corals build the reef structure that protects our coastlines from erosion and storm surge, and provides habitat, nursery areas, and food for over 9 million species of animals and plants, including commercial fish species. Coral populations typically recover after disturbances through sexual reproduction, which results in the production of coral juveniles that replenish depleted reefs. However, because the abundance of corals on the reef is currently low, the chances that eggs and sperm from different colonies will meet is severely reduced, precluding the production of offspring and subsequently the recovery of the reef through natural processes.

Reef recovery can be accelerated by increasing the density of corals on the reef through active restoration. In Florida, restoration projects are informed by research co-designed by scientists aiming to preserve and restore reef ecosystems with cost effective interventions at large spatial scales (Pienkowski et al. 2024). Increasing coral density on the reef can be achieved through coral propagation. The sexual propagation of corals can massively increase the number of genetically unique corals available for restoration and increase the genetic diversity of existing populations, potentially increasing their resilience to current and future stressors. To sexually reproduce corals *ex situ*, corals are maintained year-round in conditions that mimic the natural annual cycles of temperature, sun, and moon light (Craggs et al. 2017), which induces gonad maturation and synchronous spawning. Then, coral gametes can be collected, fertilized, developed into embryos that get reared to the larval stage, and then settled. The newly settled corals are grown until they reach a size suitable for outplanting on the reef.

This project aimed to sexually propagate corals of species affected by the stony coral tissue loss disease in KJCAP for restoration as well as conduct research to continuously improve it. The methodologies to sexually propagate corals were further optimized to reduce production time, costs, and labor – which is essential to restore coral reefs at the ecosystem scale and thus guarantee these will continue to provide coastal protection, serve as nursery habitat for important fisheries and support the tourism industry.

The individual reproductive contribution of parental coral colonies to their sexually produced offspring is a critical but poorly characterized parameter in *ex situ* coral restoration programs. Identifying which broodstock genotypes contribute gametes, and in what proportions, is essential for managing genetic diversity in land-based nurseries and ensuring that outplanted juveniles carry sufficient genetic variability for long-term reef recovery. Equally, the relationship between parental genotypes and the thermal tolerance of sexually produced juveniles remains largely unexplored, limiting the ability to identify and prioritize thermally resilient genotypes for restoration. Addressing both gaps requires integrating genomic parentage analyses with direct experimental assessments of thermal stress response in the same juvenile cohort.

Task 8 addressed these gaps with *M. cavernosa*, one of the reef-building species most impacted by SCTLD in NSU's broodstock collection, using two complementary approaches. First, DNA was extracted from 13 broodstock colonies held at NSU's land-based nursery and from nine over one-year-old juveniles produced during the 2024 spawning season and assessed using the Coral Bleaching Automated Stress System (CBASS) (Evensen et al., 2023), for acute short-term thermal challenges. All 22 samples were submitted to the University of Florida ICBR Gene Expression and Genotyping Core for whole-genome sequencing (WGS). Genome-wide single nucleotide polymorphisms (SNP) genotyping will enable parentage assignment of juveniles to broodstock genotypes and phylogenomic characterization of the broodstock cohort. Algal symbiont identity was characterized in both broodstock and juveniles samples via PCR amplification and sequencing of the chloroplast 23S rDNA (cp23S) locus (Zhang et al., 2000). Second, an acute thermal stress assay was conducted on May 12, 2026, using the CBASS protocol. Nine *M. cavernosa* juveniles were distributed across three treatment tanks — Control (26°C), CBASS-1 (+3°C, 29°C target),

and CBASS-2 (+6°C, 32°C target) — and exposed to a standardized 3-hour ramp, 3-hour hold, and cooldown profile. Photosynthetic performance (Fv/Fm) was measured at baseline, post-heat, and recovery time points using a Diving-PAM fluorometer to quantify bleaching susceptibility at the colony level.

Together, these datasets will enable the first genome-wide assessment of parental contribution to juvenile cohorts produced at NSU's land-based nursery and provide an initial characterization of whether parental genotype predicts offspring thermal resilience. This information directly supports genomic-assisted coral restoration by identifying which broodstock genotypes contribute to offspring production, by linking individual genotypes to acute thermal tolerance, and by characterizing the algal symbiont community in both parents and juveniles. These findings will inform broodstock management priorities, mating design, and outplanting decisions aimed at maximizing genetic diversity and thermal resilience in restored populations of *M. cavernosa* in the KJCAP.

Improvements to rearing conditions rely on screening physiological proxies for early life stages. A portion of this project investigates how environmental conditions and parental origin shape the metabolic performance of *D. labyrinthiformis* larvae, a critical life stage for coral population recovery and reef restoration. Coral larvae rely entirely on maternally provisioned energy reserves, and their ability to withstand thermal stress, maintain homeostasis, and complete settlement depends on how efficiently they use these reserves. Because metabolic rate governs the pace at which lipids and proteins are consumed, quantifying aerobic and anaerobic metabolism provides a powerful early indicator of larval fitness, resilience, and post-settlement potential. This work addresses a major knowledge gap in coral restoration by characterizing how temperature, glucose availability, developmental stage, and broodstock origin influence larval metabolic trajectories.

To accomplish this, larvae derived from both field-collected and nursery-spawned gametes were reared under controlled laboratory conditions and assessed using high-resolution oxygen-consumption assays and enzymatic activity measurements. These complementary approaches allowed us to quantify whole-organism aerobic metabolism alongside the activity of

key metabolic enzymes, lactate dehydrogenase, alanopine dehydrogenase, strombine dehydrogenase, and citrate synthase, that reveal the balance between anaerobic and aerobic pathways. The experimental design incorporated multiple developmental time points and two ecologically relevant temperatures (26°C and 30°C), as well as glucose supplementation trials to evaluate whether exogenous carbon sources alter metabolic demand. Together, these methods provide a comprehensive view of larvae energetic capacity and stress sensitivity.

The resulting dataset offers actionable insights into coral nursery operations and restoration planning. Field-origin larvae exhibited higher anaerobic enzyme activity and more stable metabolic increases through development, suggesting greater inherent stress tolerance. Nursery-origin larvae showed more variable metabolic patterns and a strong late-stage shift toward aerobic metabolism, indicating different energetic strategies shaped by parental environment. Temperature effects also differed by origin, with nursery larvae showing metabolic depression at 30°C during mid-development. These findings highlight the importance of broodstock conditioning, temperature management, and developmental staging in larval rearing systems. By integrating metabolic physiology into nursery decision-making, restoration practitioners can better optimize larval survival, settlement success, and long-term restoration outcomes.

In Phases I-VI of this project (PO B66DAC, PO B77DF8, PO B97E48, PO C031A6, PO C2221C, PO C3EF03) we held mature-size colonies of unique genotypes of seven reef-building coral species impacted by the disease from the KJCAP, namely *M. cavernosa, O. faveolata, P. clivosa, P. strigosa, C. natans, D. labyrinthiformis,* and *Siderastrea siderea* to preserve their genotypes, annually induced them to mature their gonads and spawn synchronously in the laboratory, raised their offspring and then outplanted them on the reef. In the process, we conducted research to improve their culture methodology to increase the number of corals available for restoration, and to reduce production time, costs, and labor. We have optimized species-specific needs in terms of food, water quality, and light which lead to increased reproductive output and synchronous spawning of resilient coral genotypes of the disease-impacted reef-building corals from the KJCAP for reef restoration efforts. We have also increased our understanding of the species biology, e.g. our cumulative annual spawning observation revealed that *M. cavernosa* is not gonochoric but instead is a bidirectional sex changer (Laforest et al. 2024). We identified processes that limit

fertilization (change in temperature and water chemistry) and applied a new technique that leads to >95% fertilization in *M. cavernosa*. We collected data and modeled the larval survival and competency dynamics of seven coral species which were integrated into bio-physical models of coral larval dispersal to assess connectivity in FCR and identify optimal sites to protect and restore. We developed a mass-scale larval and settlement system which maximizes water quality, minimizes labor, and leads to higher larval survival. We increased larval settlement rates of *O. faveolata*, which typically displays very low settlement rates (<5%) using purples tiles. Light (irradiance and spectrum) were also optimized, leading to increased survival and growth of coral juveniles.

NSU's land-based nursery has three mass-scale production systems and is currently being expanded to increase capacity. This nursery includes: 1) a Tri-ACSC (room 108A GHOC) room with four raceways that hold mature-size colonies of unique genotypes of the six reef-building coral species impacted by the disease from the KJCAP, in which different corals are induced to spawn at one of three prescribed time points, i.e. staggered spawning to optimize the use of space and equipment; 2) the Marine Larval Ecology and Recruitment (MLER) lab (room 242 GHOC) contains eight mass-scale recirculating systems for larval culture, settlement and early grow-out of corals (up to 3-4 months old), each containing a conical tank to culture the larvae connected to a raceway (equipped with lights) dedicated to settlement and early grow-out which allows a hands-free transfer of larvae to settlement trays; 3) the outdoor area contains 12 raceway tanks dedicated to the late grow-out of corals (3-4 months and older), quarantine areas, and experimentation, with 22 more tanks being added in by the end of 2026 (FCR3 Initiative funding). Additionally, congressional earmark funding is being used to renovate a room on the 5th floor of the GHOC, which will be dedicated to growing live food for corals and the larval of culture of "cleaning crew" herbivores which juvenile stages will be co-cultured with corals to control algal overgrowth and thus increase survival and accelerate growth. This new room will also include a streamlined coral micro-fragmentation station with four raceways and a workshop to build and repair structures for the offshore nursery in support of outplanting activities. The Offshore Coral Nursery serves as a biobank for genotypes across FCR and is used to propagate corals through fragmentation and provide acclimation for corals sexually produced at the NSU's Coral Nursery; this nursery has the

capacity to hold up to 11,000 corals. Through all these achievements we have been able to preserve the genetic diversity of the corals that survived the disease (potentially more disease resistant), increase the coral biomass available for future restoration projects, and increase the genetic diversity of the populations on the reef (new genotypes are formed through genetic recombination). We aimed to continue to increase the production of corals for restoration so that they can re-establish natural sexual reproduction on the reef, and hence reef recovery and resilience.

- **METHODOLOGY**
    - **Task 2: Coral spawning and gamete collection at land-based nursery (Figueiredo)**

Induction systems were programmed for staggered spawning, i.e. *M. cavernosa* were set to spawn in July/August 2025, *P. clivosa* in January/February 2026, *C. natans* and *P. strigosa* in April/May 2026 and *D. labyrinthiformis* in May/June 2026. Beginning on the full moon of all programmed spawning months (depending on species and programmed annual cycle), for up to 14 days every night after sunset, broodstock colonies that were held long term in the land-based nursery were observed for spawning. Spawning induction systems with *M. cavernosa*, *C. natans*, *O. faveolata*, *P. strigosa*, and *D. labyrinthiformis* were monitored from the programmed sunset time to 240 minutes after sunset and the system with *P. clivosa* was monitored closely between 180 minutes after sunset to 600 minutes after sunset, as these were the peak spawning time for the species documented in previous years (refer to phase IV to VI).

The time of gamete release, amount (low, medium, or high) of gametes, and identity of colonies that spawn each night was recorded. For gonochoric species, fertilization occurred within the adult tank, and the fertilized eggs (embryos) were collected 90 minutes after the last spawn by skimming the surface with a cup. For hermaphrodite species, egg and sperm bundles were collected upon spawning by skimming the surface with a cup, where gametes were placed in containers filled with tank seawater for fertilization, and then were placed floating on the adult tank to serve as water bath and thus maintain the same temperature.

- **Task 3: Fertilization, larval culture and settlement (Figueiredo)**

Eggs and sperm from colonies of each species that spawned in the land-based nursery from Task 1 were combined, keeping sperm at concentrations which maximize fertilization. One hour after the eggs were pooled with the sperm, the eggs were washed through a series of dilutions using gravy separators to remove the sperm and avoid polyspermy. We used four replicate mass-scale larval culture and settlement recirculating systems to rear the embryos to larvae, settle them on ceramic substrates, and grow the newly settled corals until they reached 3-4 months old. Each system had two 95L conical tanks modularly connected to two raceways that shared the same recirculating water via a shared sump. Specifically, embryos were reared to the larval stage in a 95L conical recirculating system. Once the larvae started swimming (all at least rotating, with a small percentage swimming directionally), the filters on the outflow of the conical tanks were removed and the larvae flowed into settlement trays (without handling) placed inside the raceway.

The bottom of the settlement trays were covered with settlement tiles which were pre-conditioned for two months in the outdoor tanks and sprinkled with crushed crustose coralline algae to induce larval settlement and metamorphosis. These recirculation systems were equipped with mechanical, biological, and chemical filtration, UV sterilizer, calcium, and phosphate reactors, heaters, and chillers. Given there are four mass-scale larval culture systems (eight raceways), this setup allowed us to rear large quantities of corals. The temperature, pH, and salinity levels mimicked historical conditions on the reef during a typical summer (not necessarily current conditions) to maximize survival. Water changes were performed as needed to avoid toxic components such as ammonia accumulating and harming the larvae.

After the competent larvae were exposed to the conditioned tiles for one to two weeks, the tiles were inspected under the microscope for metamorphosis. Any tiles with settlers were placed back in the recirculating tank for further grow-out.

- **Task 4: Grow-out of the newly settled corals in the land-based nursery (Figueiredo)**

Newly settled corals were reared in four 1500L indoor recirculating systems until they reached 3-4 months old. Each of these systems are composed of two raceways (each 2.5 x 0.6 x 0.3 m) with a flow rate of 350L/h and shared sump equipped with mechanical, biological and chemical filtration, UV sterilizers, heaters and chillers, calcium and phosphate reactors, and Radion LED lights. Newly settled corals have a very small environmental tolerance range to environmental conditions; thus, it was extremely important to maintain optimal environmental conditions, paired with stable water quality, and provide varied food *ad libitum*.

Corals were reared at a constant 27°C to promote growth without causing thermal stress. Temperature was measured daily with a YSI® Pro30 temperature probe to ensure accuracy. The lights followed a natural photoperiod with light irradiance increasing from sunrise until solar noon (when maximum irradiance is reached) and decreasing after that until sunset. We used a light spectrum that mimicked the spectrum at reef depth (around 10m). Newly settled corals are very sensitive to high light irradiance levels and grow faster under lower irradiance levels; however, once coral can feed heterotrophically and symbiosis is fully established, they require higher light levels to survive and grow. Previous experiments identified the optimal light levels for *M. cavernosa* and *O. faveolata* to be 10 µmol photons.cm^{-2} sec^{-1} during Weeks 1-4, 40 µmol photons.cm^{-2} sec^{-1} during Weeks 5-8, 60 photons.cm^{-2} sec^{-1} during Week 9, 80 µmol photons.cm^{-2} sec^{-1} during Week 10, 120 µmol photons.cm^{-2} sec^{-1} during Week 11, 140 µmol photons.cm^{-2} sec^{-1} during Week 12, and 180 µmol photons.cm^{-2} sec^{-1} onwards.

The salinity was maintained at 35 ppt. Reverse osmosis water was added daily to the sump to replace evaporated water and maintain salinity. Water quality tests were performed weekly to determine calcium, alkalinity, ammonia, nitrite, nitrate, and phosphate concentrations. If necessary, partial water changes will be performed to ensure the water does not contain ammonia or nitrites. Ideal nitrate values are 2-3 ppm and phosphate at 0.4-0.5 ppm. Nitrates should be about 6.7 times higher than phosphates.

Adult corals of the several species were placed in the same tank to release algal symbionts and facilitate symbiont acquisition by the coral juveniles. Corals were hand-fed daily Reef-Roids (PolypLab), Golden Pearls (5-50 µm, Aquatic Foods Inc.), Selcon (American marine Inc.), and Coral aminos (Brightwell Aquatics) *ad libitum* to enhance survival rates and promote growth. Overgrowth by algae was controlled with the help of small herbivorous animals, such as snails and hermit crabs, and manually mitigated to minimize coral mortality and promote growth. At the 6-month age mark the number of corals of each species was counted.

NSU also received coral recruits from The Florida Aquarium (TFA) on March 31st, 2026, and University of North Carolina Wilmington (UNCW) on April 22nd and May 26th, 2026. All coral juveniles that are currently being reared at the land-based nursery will remain in our care until they reach a size suitable to be moved to the offshore nursery (refer to Task 5).

- **Task 5: Preserve coral genotypes of disease impacted species and induce gonad maturation and spawning in captivity (Figueiredo)**

NSU's land-based nursery held an extensive number of colonies of the reef-building coral species to preserve their genotypes *ex situ* (genotype banking/caching), specifically 30 *M. cavernosa,* 10 *O. faveolata*, 19 *P. clivosa,* 18 *P. strigosa,* 20 *C. natans*, 20 *D. labyrinthiformis*, and 15 *S. siderea* colonies of unique genotypes, all from the KJCAP (132 colonies total). These colonies represent a significant part of the genetic diversity of the populations of these species in the KJCAP. Importantly, these genotypes survived the disease event and thus possibly are more disease-resistant than genotypes from other areas along Florida's Coral Reef. All healthy, mature-size colonies of *M. cavernosa, O. faveolata*, *P. clivosa, P. strigosa, D. labyrinthiformis,* and *C. natans*, were maintained in four indoor independent recirculating tanks (room 108A GHOC) under conditions that mimicked the historical temperature, photoperiod, and solar/lunar irradiance and spectrum on the reef to induce their gonads to mature and spawning to occur synchronously; we then used their gametes to produce offspring that perpetuated but also recombined their genes into new genotypes (Task 1).

The indoor systems are fitted with a web-based microprocessor (Neptune Systems, Apex) attached to the tank and outfitted with Radion LED lights. Using Apex classic dashboard, the target seasonal temperature was programmed and using the Mobius app; the photoperiod and lunar cycle data has been programmed. Annual variation in sea temperature on the reef was based on HOBO temperature loggers (HOBO Pro V2) data collected at the Southeast Florida Coral Reef Evaluation and Monitoring Project (SECREMP) sites between February 2007 and June 2016. Data points for periods with cold snaps and/or bleaching events were removed, and the remaining data was used to create an average profile of the annual temperature cycle in the region. Sunrise, sunset, moonrise, and moonset times were downloaded from www.timeanddate.com. To simulate annual variation in photon intensity, irradiance averages recorded by NASA Surface Meteorology and Solar Energy for the reefs off Fort Lauderdale were averaged and converted into data for LED programming.

Both indoor and outdoor systems were equipped with mechanical, biological, and chemical filtration, UV sterilizers, heaters and chillers, calcium and phosphate reactors and/or automatic dosers. Corals were target-fed Golden Pearls (200–500-micron, Aquatic Foods Inc), Reef-Roids (PolypLab), and Polyp Booster (PolypLab) *ad libitum* to promote growth and enhance survival rates. Any unhealthy (quarantine) or immature-size colonies of the other coral species were maintained in outdoor tanks. Coral colony health was classified monthly by conducting visual assessments of live tissues to determine if the colony is healthy, unhealthy, or deceased. Any new corals added to the collection will be subsequently added to the effort, photographed, and assessed for colony condition thereafter. Water quality tests were performed weekly to determine alkalinity, calcium, ammonia, nitrite, nitrate, and phosphate concentrations. If necessary, partial water changes were performed to ensure the water did not contain ammonia or nitrites. Nitrates are held at 2-4 ppm, and phosphate at 0.2-0.5 ppm. To ensure there were no detectable levels of trace metals or other trace elements, ICP-OES testing was submitted twice per year per system.

Holding corals of disease impacted species to induce gonad maturation and spawning in captivity has previously been funded by DEP.

- **Task 6: Grow-out of coral juveniles at the offshore nursery (Gilliam)**

Up to 1,000 coral juveniles of stony coral tissue loss disease susceptible species (*M. cavernosa, O. faveolata, P. clivosa, P. strigosa, C. natans,* and/or *D. labyrinthiformis*) were moved to the offshore nursery in late fall 2025 and early 2026. These coral juveniles were deployed on suspended tree structures and/or modules. Colony planar images and size (diameter) were taken of the 25% subset at the time of deployment to the offshore nursery. Colony planar images, size, and condition were monitored at approximately 1 week, 1-month, and 3-months after deployment in the nursery for this 25% subset.

The surviving coral juveniles moved to the offshore nursery in January 2025 (funded under Phase VI in FY 2024-25) were moved to the nursery for grow-out and outplanted in fall 2025 and early 2026. The exact number of outplants was dependent upon the survival and health condition of the corals moved to the nursery. Outplant colony survival and condition were monitored at approximately 1 week, 1-month, 3-months, and 6-months after deployment. During each monitoring event, coral colony conditions were recorded for all corals. Representative coral images were taken during each monitoring event, and planar images were taken of at least 25% of the corals at the time of deployment and 6 months after deployment.

Annual efforts to transfer coral juveniles and microfragments from the land-based nursery to the offshore nursery started in late 2020/early 2021. Surviving corals in the offshore nursery in the fall of each year were outplanted. Previous funding included the cost of monitoring these corals for up to 6 months post-outplanting. To gain information on long-term survival, all previous outplant sites were visited in Fall 2025 and colony conditions were recorded for all surviving colonies. Planar images were taken of the surviving corals from each outplant year.

A FL FWC SAL was received prior to outplanting in Fall 2025. SALs permit the collection, microfragmentation, and grow-out of SCTLD-susceptible corals, pending health certification, and release authorization. The permitting agency (FWC) has indicated they will continue to permit these activities.

- **Task 7: Settlement trials with CYPRO (Figueiredo & Schupp)**

Coral larvae settlement, a key mechanism of coral population replenishment and recovery, has been largely understudied. CYPRO has been shown to promote >95% coral settlement and metamorphosis of coral species from the Pacific (Fiegel et al. 2023; 2025[LF1] , Petersen et al. 2023). CYPRO is actively harvested and subsequently enriched along the ectoderm of larvae of the scleractinian coral. Then, a light-dependent reaction transforms the CYPRO molecules through photolytic decomposition and provides a constant supply of hydrogen peroxide (H_2O_2), leading to attachment on the substrate and metamorphosis into a coral polyp.

Following the methodology described in Petersen et al. (2023), we tested if CYPRO can induce settlement and metamorphosis of coral species from the KJCAP. Coral larval settlement at land-based nurseries is currently very low (ca. 20%), thus immediately reducing coral production to a fifth. Relative to other products, such as tetrabromopyrrole (TBP) which degrades within hours, this product has the advantage of remaining stable over time (if kept in a dark container) and thus being able to be shipped and stored to be used whenever required.

- Well Plate Experiments

The trials were conducted by comparing the percentage of larvae settling and metamorphosing in different concentrations of CYPRO relative to a negative control (0.2µm filtered sea water (FSW)) and a positive control (POS) which represented a commonly used settlement cue, crustose coralline red algae (CCA) collected from the walls of a cultivation tank. For this experiment, we targeted *D. labyrinthiformis* larvae 2, 6 and 9 days after spawning. Each treatment was conducted using six replicates of 10 larvae each.

CYPRO, dissolved in methanol (MeOH), was pipetted on the bottom of the 6 well plate. After the evaporation of the MeOH, FSW was added. Since CYPRO is not water soluble, it remained on the bottom of the well.

To start the experiments, swimming larvae were added and placed in a 12h dark/light rhythm. Light was set at approx. 60 PAR with a peak wavelength at approx. 450nm. After 48 hours, larvae were monitored for settlement using a binocular. Stable attachment was confirmed by blowing a gentle pipette stream against settled larvae.

- PRIMING Experiments

For both PRIMING experiments *D. labyrinthiformis* larvae, 2 days after spawning, were used. After the evaporation of the MeOH, FSW was added. In experiment (A), 6 replicates with 10 larvae each, in experiment (B) 9 replicates with 5 larvae each were used. Larvae were exposed to CYPRO for (A) 10 hours and (B) 11 hours in dark conditions. After the pre-condition period, larvae were transferred into 6 well plates without CYPRO for settlement, set in a 12 h light/dark rhythm. Settlement was scored during the transfer period and after 48 hours experiment duration.

- **Task 8: Genome-wide parentage analysis and thermal stress response of parental colonies (Gomez-Corrales and Liberman)**

The individual reproductive contribution of parental colonies to their offspring remained to be studied at NSU. To address this gap, we aimed to use WGS of both broodstock colonies and offspring from one priority coral species as proof of principle to perform parentage analysis based on hundreds of thousands of SNPs. This high-resolution genotyping analysis clarified the genome-wide contributions of parental genotypes to sexually produced coral juveniles, allowing us to estimate the effective population sizes of broodstock as well as their overall genotypic diversity. Additionally, algal symbiont genotyping using sequencing of the chloroplast DNA was performed to determine dominant variants in both parents and juveniles. Symbiont cp23S sequences from broodstock and juveniles were aligned with GenBank references using MAFFT, and a maximum-likelihood tree was inferred in IQ-TREE with automatic model selection and ultrafast bootstrap support; the tree was visualized in R (ggtree).

Furthermore, we used CBASS to assess the thermal stress response of sexually produced juveniles from the last 2025 spawning event, measuring their bleaching response under acute short term temperature stress conditions. The bleaching response was measured with a diving-PAM

fluorometer to evaluate the integrity of the symbionts' photosynthetic machinery. While CBASS provides a rapid experimental framework, it can simulate the acute thermal anomalies typically experienced in natural reef environments (Voolstra, 2022). By integrating genomic data with bleaching susceptibility, this study provided insights into the genetic architecture and symbiont associations underlying thermal tolerance, informing coral restoration strategies to enhance reef resilience and support broader genomic-based restoration approaches for other species in our nurseries.

- Coral Bleaching Automated Stress System (CBASS)

Temperature in each tank (45 L cooler, with ~16 L of artificial seawater) was maintained to within ±0.1°C by a thermostat system (Apex A3 Aqua Controller, Neptune Systems) using two IceProbe Thermoelectric Aquarium Chillers (Nova Tec), tank cooling fans (LONDAFISH Aquarium Chillers), and one heater (100 W Titanium Heater Element, Bulk Reef Supply). Light was controlled via the myAI app using full-spectrum aquarium lamps (Hydra TwentySix HD LED) on a sunrise-to-sunset day/night cycle at a photosynthetically active radiation (PAR) of ~180 µmol photons m^{-2} s^{-1}, closely matching PAR levels in the nursery at sunset on a clear day. Water flow and oxygenation were maintained via a constant drip of artificial seawater; each tank was also fitted with a wavemaker pump (SunSun JVP-110, 528 GPH) and an airstone (Uniclife Aquarium Air Pump Dual Outlet) to ensure constant water motion and oxygenation. Temperature was additionally logged with a HOBO Pendant® Temperature/Light MX2202 Data Logger placed in each tank.

- Temperature Monitoring

Temperature was recorded continuously in each tank using HOBO MX2202 pendant loggers (Onset Computer Corporation; ±0.2°C accuracy) at 2-minute intervals and an Apex A3 aquaculture controller probe (Neptune Systems; ±0.1°C accuracy) at 10-minute intervals. HOBO 2-minute records were resampled to 10-minute means by averaging all readings within each 10-minute window to match the Apex logging interval. All timestamps were recorded in Eastern Daylight Time (EDT, UTC−4). HOBO data exported from HOBOconnect were handled with force_tz() in R (lubridate package) to correct the UTC offset rather than converting time zones, as the export stores local clock time labelled as UTC.

Phase-level descriptive statistics (mean ± SD, min, max) were computed for five experimental phases: Baseline (20:00 May 11 – 12:00 May 12), Ramp-up (12:00–15:00), Hold (15:00–18:00), Cool-down (18:00–19:00), and Overnight (19:00 May 12 – 08:00 May 13). For Figures 12 and 13, the HOBO A+B mean and Apex series are plotted separately; Figure 14 pools all available sensors per tank per 10-minute interval before computing phase summaries, so its SD reflects both temporal variation within each phase and inter-sensor spread. Warming and cool-down rates were computed as (end temperature − start temperature) ÷ elapsed hours within the respective phase windows. Return-to-ambient times were defined as the first 10-minute interval at or below 26°C following the end of the hold period. Apex probes were calibrated against a YSI Professional Series reference on May 8, 2026 at operating temperature (26°C). All temperature analyses were conducted in R (≥4.3) using the tidyverse, lubridate, xml2, and readxl R packages.

- PAM Fluorometry

Photosynthetic efficiency (Fv/Fm) was measured with a Diving-PAM fluorometer (Walz) under dark-adapted conditions (minimum 20 minutes). Baseline measurements were collected on four separate dates (May 5, 6, 7, and 11, 2026); when multiple readings for the same colony were obtained on a single date, values were averaged to produce one daily mean per colony. The four daily baseline means per colony were averaged to a single pre-experiment value for the mixed-effects model. Post-heat measurements were collected on May 12 following removal of colonies from the CBASS tanks, and recovery measurements on May 13 following overnight return to ambient temperature.

Treatment-level effects across phases were assessed with a linear mixed-effects model (Fv/Fm ~ Phase × Treatment + (1|Colony)) fitted using lmerTest in R. Colony was included as a random intercept to account for repeated measurements on the same individual. Pairwise phase contrasts within each treatment were evaluated using estimated marginal means (emmeans package, version ≥1.8) with Tukey correction for multiple comparisons. Colony-level significance

was assessed separately using one-sample t-tests comparing each colony's post-heat or recovery Fv/Fm value against its own baseline distribution. All PAM analyses were conducted in R (≥4.3).

- **Task 9: Assessing energetics of coral early life stages and breeding stock to enhance nursery efficiencies (Martinez)**

- Larvae sourcing and maintenance

Larval populations consisted of *D. labyrinthiformis* larvae from field-collected gametes (5/12/26) as well as nursery-collected (5/15/26) individuals. Each source was assayed separately during the experiments. Both larvae populations were subsampled from corresponding rearing tanks and transferred to the animal physiology laboratory, where they were held in 2.0 liter water-jacketed cylindrical chambers connected to a recirculating water bath set at 26.33 ± 0.51°C (mean ± stdev) at densities no higher than 1 larva/mL. The temperature-controlled chambers (2 total) were gently moved via an orbital shaker, set at 75rpm over the entire rearing period (72hrs). Approximately 300 larvae from field- collected gametes of *D. labyrinthiformis* were subsampled from the rearing chambers at early (24hrs post-fertilization) and late (48-72hrs post-fertilization) developmental stages and stored in 0.2µm-filtered seawater (FSW) at -80°C for enzyme analysis.

- Glucose exposure of nursery gamete-derived *D. labyrinthiformis* larvae

A subset of 60 larvae at approximately 30 hours after fertilization were subsampled from the rearing chambers and placed in 15mL conical tubes containing either FSW or FSW + 10mM glucose, at a density of 1 larva/mL. Three, 10 mL replicates per treatment with 10 larvae each were maintained for 72 hrs at 26.33 ± 0.51°C, with 24hrs media change to ensure reduced waste buildup and stable glucose concentration. At the end of the 72hrs incubation period, larval samples were placed in respirometry chambers for metabolic rate measurements.

- Oxygen consumption measurements

Metabolic screening was carried out using indirect calorimetry, where oxygen consumption is monitored under controlled conditions. A total of 2 individual larvae were pooled per respirometry sample into a 2 mL sealed glass chamber, to ensure a detectable and reliable metabolic signal. The larvae were contained in 0.2 µm filtered seawater (FSW), a critical step to eliminate confounding background microbial respiration that can otherwise bias measurements in small-volume systems (Ikeda et al., 2000).

Oxygen concentration in the sealed chamber was monitored every 1-2 hours external to the chamber via a fiber optic cable connected to a PreSens Fibox4 monitoring system. The fiber optic cable probed a 3mm diameter optical sensor (PreSens pst-3), which lies inside each glass chamber. These micro-optodes are superior to traditional polarographic electrodes for larval studies because they do not consume dissolved oxygen during the measurement process, ensuring higher sensitivity and stability in micro-chambers (Agostini et al., 2013; Edmunds et al., 2011; Okubo et al., 2008). Each O_2 optic sensor or optodes were calibrated for each assay temperature via two point calibration; saturating oxygen FSW at recorded temperature and pressure, and the signal corresponding to zero oxygen in the presence of sodium dithionite.

Oxygen consumption rates were calculated from the depletion of oxygen over a 3-4 hour period using the slope of a simple linear regression during stable incubation intervals once the larvae have acclimated for 30 min to the chamber conditions (Ikeda et al., 2000). Oxygen consumption rates with a linear regression exhibiting a coefficient of determination (R^2) ≤ 0.85 were considered atypical and removed from further analysis. A total of 9 chamber replicates were carried per temperature treatment, and two temperature treatments (26°C and 30°C) were tested to calculate the reaction norm of aerobic metabolism and temperature. A blank chamber filled only with FSW was also monitored for background oxygen consumption, which was later subtracted from each run. All runs were carried in dim light conditions.

- Enzymatic activity measurements

Frozen tubes containing tubes containing 100 larvae each were thawed on ice, centrifuged, supernatant discarded and pellet containing larvae washed with 1.0mL ice-cold homogenization buffer containing 50 mM imidazole (pH 7.8) (Sigma-Aldrich) and 0.1 mM phenylmethylsulfonyl fluoride (PMSF) (Sigma-Aldrich). Each larval sample was resuspended in 500µL of homogenization buffer and sonicated (70 kHz,) for 30 sec. The samples will be centrifuged (10,000 RPM, 20 min, 4 °C) and the sample supernatant will be used as an enzymatic source. Measurements were performed in a UV/VIS Spectrophotometer at room temperature.

Lactate dehydrogenase (LDH) activity was measured in a reaction solution containing 0.2 M imidazole (pH 8.0), 5 mM sodium pyruvate and 0.15 mM nicotinamide adenine dinucleotide (NADH) (Sigma-Aldrich). LDH activity was initiated by adding 20 µL of the sample supernatant in 330 µL of the reaction solution and monitored at 340 nm.

The citrate synthase (CS) assay was performed in reaction solution containing 50 mM 4-(2-hydroxyethyl)-1- piperazineethanesulfonic acid (HEPES), 0.1 mM acetyl-CoA and 0.1 mM dithionitrobenzoic acid (DTNB) (Sigma-Aldrich). The background activity was monitored by adding 10 µL of the sample supernatant in 290 µL of the reaction solution. CS activity was initiated by adding 50 µL of 3.5 mM oxaloacetic acid (Sigma-Aldrich) (final concentration 0.5 mM) and monitored at 412 nm.

Strombine dehydrogenase activity was assessed by preparing a 1 mL reaction mixture containing 50 mM imidazole buffer (pH 7.0), 0.2 mM NADH, 10 mM pyruvate, and 10 mM L-serine. Sample supernatant (50 µL) was added to initiate the reaction, and the mixture was gently mixed before the decrease in absorbance at 340 nm is recorded for 3–5 minutes. Enzyme activity was calculated from the rate of NADH oxidation using an extinction coefficient of $\varepsilon = 6.22\ mM^{-1} \cdot cm^{-1}$.

Alanopine dehydrogenase activity was measured by preparing a 1 mL reaction mixture containing 50 mM imidazole buffer (pH 7.0), 0.2 mM NADH, 10 mM pyruvate, and 10 mM Lalanine. Sample

supernatant (50 μL) was added to initiate the reaction, and the mixture was gently mixed by pipetting before the decrease in absorbance at 340 nm is recorded over 3–5 minutes. Enzyme activity was calculated from the rate of NADH oxidation using an extinction coefficient of ε = 6.22 $mM^{-1} \cdot cm^{-1}$.

During enzyme activity trials, the instrument was calibrated to account for instrumental drift and residual absorbance of cuvettes. The control activity (reaction solution without enzymatic source) was determined in the LDH and CS assays. Enzymatic activity was normalized by homogenate protein concentration using a commercial reagent kit based on the Bradford method (Bradford Reagent, Sigma-Aldrich). Final enzymatic activity was expressed as units (U) mg $protein^{-1}$. Measurements of enzyme activity and protein concentration were technically replicated for each individual sample (n = 2) for double-checking.

- Statistical analysis

Statistical analyses were conducted to evaluate how temperature and source population influenced metabolic performance. Whole-organism metabolic rate data were analyzed using a two-way ANOVA to test for main and interactive effects of origin (field-collected vs. nursery gamete-derived larvae) and temperature. To further assess developmental dynamics, differences in metabolic rate as a function of developmental time and temperature were evaluated independently for each larval source using separate two-way ANOVAs, followed by Holm–Sidak post hoc multiple comparison tests when significant effects were detected.

Glucose-specific metabolic rate responses to temperature were likewise analyzed using a two-way ANOVA, with Holm–Sidak pairwise comparisons applied to resolve differences among temperature treatments. Enzyme activity data were analyzed using a two-way ANOVA to test for main and interactive effects of origin (field-collected vs. nursery gamete-derived larvae) and developmental time (early vs. late) All values reported are mean ± SEM.

- **RESULTS**
    - **Task 2: Coral spawning and gamete collection at land-based nursery (Figueiredo)**

- *Montastraea cavernosa* Summary

From July to August 2025, spawning was observed in a total of 10 *M. cavernosa* colonies held within the induction systems at NSU's land-based coral nursery. The induction systems were prescribed real time temperature, solar and lunar cues; there was no seasonal phase shifting on the programming for this species. Colonies were monitored across historically proven peak spawning nights, i.e. across the 6th to the 11th day after the programmed full moon. Systems with *M. cavernosa* were closely monitored 90 minutes before the programmed sunset time until 240 minutes after sunset (MAS).

In July 2025, on the ninth day after the full moon (DAFM), four colonies, two females and two males, released gametes between 68 minutes before sunset to 166 MAS. Colonies released closer to sunset than expected.

Following the 2025 August full moon, nine colonies, five males and four females, spawned. Spawning was observed on August 17th, corresponding to eight days after the full moon of August. Corals spawned between 0 MAS to 141 MAS.

- *Orbicella faveolata* Summary

Orbicella faveolata colonies were monitored across the 5th to 9th day after the programmed full moon from July to August 2025. The expected peak window for the *O. faveolata* colonies in the induction system was between the 5th and 7th DAFM. Colonies were monitored between 75 and 305 MAS. No spawning was observed.

- *Pseudodiploria clivosa* Summary

Pseudodiploria clivosa naturally spawns in August and September. To initiate a staggered spawning schedule and induce the corals of this species to spawn in January/February in the Tri-ACSC, this year their gametogenic cycle had to be extended by 7 months (i.e. temperatures were held steady for 7 months starting on the third month of their gametogenic cycle and then returned to mimic natural environmental cues).

Following the full moon in January and February 2026, *P. clivo*sa colonies were monitored across from the 6th to 12th DAFM starting 190 MAS until 275 MAS. No spawning was observed during this time.

- *Pseudodiploria strigosa* Summary

Broodstock of *P. strigosa* experienced an extended gametogenesis cycle, similar to the *P. clivosa* colonies. Colonies were expected to spawn from April to June 2026. Broodstock in the induction system were monitored 5 to 13 DAFM, starting –18 MAS until 238 MAS. No spawning was observed.

- *Colpophyllia natans* Summary

Colpophyllia natans colonies were monitored April to June 2026 for spawning 5 to 12 DAFM. Monitoring occurred from 0 to 190 MAS. No spawning was observed.

- *Diploria labyrinthiformis* Summary

Diploria labyrinthiformis colonies have been maintained under a 12 month, natural cycle, and were monitored for spawning from April to June 2026. Colonies were monitored 9 to 12 DAFM. Following the May 1, 2026, full moon, 4 different colonies released a small number of bundles 13 to 14 DAFM. Spawning was observed between -151 MAS and 31 MAS.

Fig 1. Student in Dr. Figueiredo's lab collecting *D. labyrinthiformis* bundles from the surface of the water with a cup.

Spawning was observed in 18 out of 20 *D. labyrinthiformis* colonies in the field at NSU's Spawning Hub between May 11th and 12th. Gametes were collected and brought to the lab for fertilization.

- **Task 3: Fertilization, larval culture and settlement (Figueiredo)**

- *Montastraea cavernosa* Summary

Attempts at fertilization were conducted when two or more colonies of *M. cavernosa*, where both sexes were represented, spawned within two hours of each other. With two days of spawning activity, there were only two attempts at fertilization across the whole spawning season for *M. cavernosa* corals. In July, one day of spawning from both sexes occurred; however, there was very little fertilization given the corals spawned asynchronously. On August 17th, where colonies of both sexes spawned, fertilization was attempted and was successful. Both spawning days this season started with a female colony releasing first; when sperm became available, a fertilization attempt was made via batch crossing all available gametes from all parent colonies. Gametes were

left to fertilize for one hour. Eggs were monitored to check for any sign of fertilization. Once cell division was observed, excess sperm was removed, and fertilization was scored. We obtained 57% fertilization success from 4 *M. cavernosa* colonies on August 20th.

The embryos were gently placed into a rearing tank to complete larval development. When the larval stage was achieved, larvae were drained from the larval rearing tanks into settlement trays in the same recirculating system filled with squared ceramic tiles (3 cm x 3 cm), sprinkled with finely ground CCA to induce settlement. These tiles were pre-conditioned for at least 6 weeks in tanks with healthy adult colonies to develop bacterial biofilms which act as another inducing settlement cue. Tiles were checked for newly settled corals one week later. Settlement proved successful for this species in August 2025, with 4 tiles with *M. cavernosa* settlers. Adult coral colonies of the same species were added to the recirculating system raceway to facilitate the acquisition of algal symbionts. Coral recruits were monitored for their general condition and survival over time.

- *Diploria labyrinthiformis* Summary

The Coral Reef Restoration and Monitoring (CRRAM) Lab at NSU observed spawning in the field on May 11th and 12th, 2026 from 18 colonies at the NSU Spawning Hub. Bundles were collected and brought to the MLER lab for fertilization. Over 630,000 larvae were produced. More than 360,000 larvae were then donated to other facilities including TFA, Secore, Mote Marine Laboratory, Smithsonian Marine Station at Fort Pierce, the Frost Museum of Discovery and Science, as well as other labs at NSU. Fertilization of the *D. labryrinthiformis* larvae from the field was successful with 95% fertilization occurring in the lab.

Spawning in the Tri-ACSC occurred on May 14th and 15th, 2026. The bundles that were released were atypical and had low fertilization in the lab. On May 14th, there was 40% fertilization and May 15th there was 65% fertilization.

Once the larval stage was achieved, larvae were drained from the conical tanks into settlement baskets that were filled with ceramic tiles sprinkled with CCA. Tiles were checked two weeks later for settlement; 216 tiles had settlers. Adult *D. labyrinthiformis* colonies were added to the raceways for symbiont acquisition. Coral recruits are actively being monitored for growth and survival. There are currently 135 tiles with *D. labyrinthiformis* settlers.

- **Task 4: Grow-out of the newly settled corals in the land-based nursery (Figueiredo)**

Corals were maintained on tiles in the indoor systems for 3 months post-settlement and then moved outside for continued grow-out (Figure 2). The tiles were cleaned regularly to minimize algal growth and ensure proper space for the corals to grow. The tiles were then nipped, and individual corals were placed onto plugs using reef glue and epoxy. This was done to isolate the individuals and reduce competition for space. New diagonal racks were assembled and installed across two tanks in the outdoor nursery, T1 and B, which increased the holding capacity. Currently, there are 15 *M. cavernosa* juveniles from the 2024 spawning season and 987 *P. strigosa* and 140 *C. natans* from the 2025 spawning season being held in T1.

Fig 2. Juvenile corals on diagonal racks after being nipped and secured on plugs in tank C.

At the beginning of March, the lab coordinated a coral transfer with TFA. Members of the lab picked up 994 plugs with individual *D. labyrinthiformis,* 50 tiles with multiple *P. strigosa* per tile and 140 tiles with multiple *C. natans* per tile all from the 2025 spawning season and placed them in tanks C and F for quarantine. Using Gryphon bandsaws and tile nippers, the *P. strigosa* and *C. natans* tiles were cut to isolate individuals and reduce competition. The individuals were then placed on plugs using reef glue and epoxy. From this donation, there are currently 847 *D. labrinthyformis,* 310 *P. strigosa,* and 541 *C. natans* on plugs in the outdoor nursery.

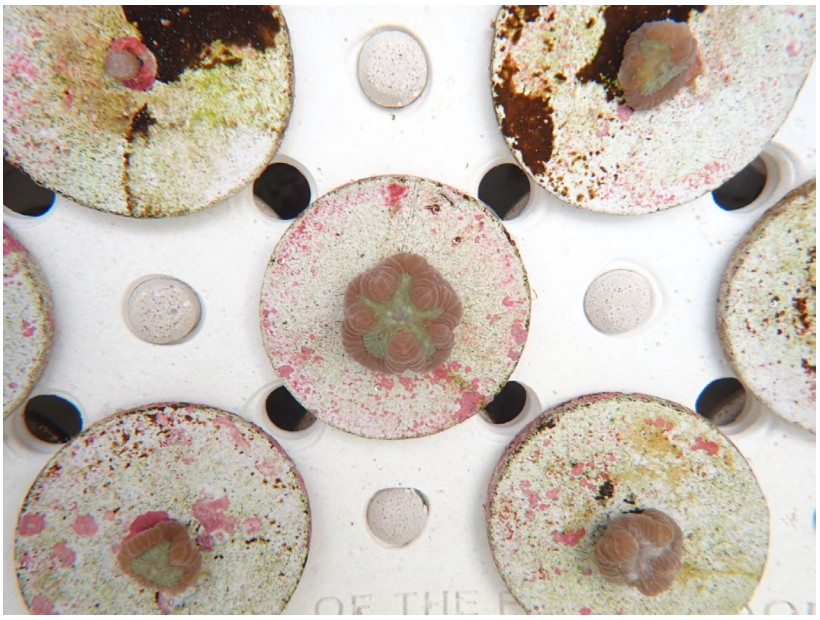

Fig 3. *Diploria labyrinthiformis* on plugs from TFA donation on March 31st.

UNCW donated 90 plugs of *M. cavernosa* from the 2024 spawning season on April 23rd and 90 plugs of *P. clivosa* from the 2023 spawning season on May 26th. Upon arrival, the *M. cavernosa* plugs were placed into tank D and the *P. clivosa* plugs were placed into tank A for quarantine. All juveniles from UNCW are doing well.

In sum, we are growing over 3,000 corals for future outplanting efforts and have grown 785 this year that were already outplanted.

For all tanks, daily water temperature and salinity measurements are recorded, and weekly measurements are taken for alkalinity and calcium. Magnesium is tested once a month. The juveniles are fed daily with a mixture of Coral Aminos, 5-50 and 50-100-micron Golden Pearls, and Reef Roids.

Table 1. Number of coral recruits produced during the 2024 spawning season that were successfully reared at the land-based nursery and transferred to the CRRAM lab as of June 2026.

Species	**Total moved to offshore nursery**
Colpophyllia natans	273
Pseudodiploria clivosa	175
Montastraea cavernosa	149
Pseudodiploria strigosa	140
Diploria labyrinthiformis	27
Siderastrea siderea	24
Orbicella faveolata	6
Total	**785**

- **Task 5: Preserve coral genotypes of disease impacted species and induce gonad maturation and spawning in captivity (Figueiredo)**

This year 132 coral colonies were held across four indoor raceways and up to twelve outdoor raceways. In July 2025, there were a total of 29 *M. cavernosa*, 16 *P. strigosa*, 19 *P. clivosa,* 10 *O. faveolata*, 17 *C. natans,* 16 *D. labyrinthiformis,* and 15 *S. siderea* in the nursery. Today, there are 29 *M. cavernosa*, 10 *P. strigosa*, 18 *P. clivosa,* 10 *O. faveolata*, 17 *C. natans,* 19 *D. labyrinthiformis,* and 5 *S. siderea*. Fourteen adult corals were vet checked and outplanted by the CRRAM lab this fiscal year. In January, the lab received nine Florida Reef Tract Rescue Project corals from Jenkinson's Aquarium. They were placed into quarantine for one month and then were moved into their current systems.

In July 2025, adult broodstock from the six priority species (*M. cavernosa, P. strigosa, P. clivosa, O. faveolata, C. natans,* and *D. labyrinthiformis*) either remained in their aquaria or were moved into one of four spawning induction systems at the start of the year. Each indoor recirculating system has one 8'x4'x16" raceway connected to a common filtration sump and receives artificial overhead lighting, whereas the outdoor recirculating systems (dimensions approx.: 10'x3'x3') connected to a common filtration sump, receive natural sunlight (reduced by shade cloth to mimic

light levels at reef depth). The indoor tanks with adult corals are named Eugene, Eddie, Echo, and Eevee. The outdoor tanks are named A, B, C, D, E, F, G, H, 1,2, 3, and 4.

All adult coral colonies were monitored daily for changes to health conditions and prescribed treatments as needed until recovery occurs (Table 2). For all species, coral health remained good during the year, suggesting the water quality is suitable for these species. Each year we find that health tends to decline post spawning for many colonies. Due to this, treatment supplies were bought in advance to aid in health recovery over time. Unhealthy colonies were typically treated with hydrogen peroxide, Revive, or Restor dips. In extreme cases, amputations were done to isolate the disease.

Table 2. Health status of all colonies maintained at the land-based nursery from July 2025 to June 2026 (H– Healthy, Green; U – Unhealthy, Yellow; D – deceased, Red; N – New Coral, Blue; O-Outplanted, Pink; CNAT– *Colpophyllia natans*, DLAB– *Diploria labyrinthiformis*, MCAV– *Montastraea cavernosa*, PSTR– *Pseudodiploria strigosa*, PCLI– *P. clivosa*, OFAV– *Orbicella faveolata* and SSID– *Siderastrea siderea*).

Species	Coral ID	Jul	Aug	Sept	Oct	Nov	Dec	Jan	Feb	Mar	Apr	May	Jun
CNAT	CN20_01R	H	H	H	H	H	H	H	H	H	H	H	H
CNAT	CN20_02R	H	H	H	H	H	H	H	H	H	H	H	H
CNAT	CN20_03R	H	H	H	H	H	H	H	H	H	H	H	H
CNAT	CN20_04R	H	H	H	H	H	H	H	H	H	H	H	H
CNAT	CN20_05R	H	H	H	H	H	H	H	H	H	H	H	H
CNAT	CN20_06R	H	H	H	H	H	H	H	H	H	H	H	H
CNAT	CN20_07R	H	H	H	H	H	H	H	H	H	H	H	H
CNAT	CN21_01	H	H	H	H	H	H	H	H	H	H	U	U
CNAT	CN21_02	H	H	H	H	U	H	H	H	H	H	H	H

Species	Coral ID	Jul	Aug	Sept	Oct	Nov	Dec	Jan	Feb	Mar	Apr	May	Jun
CNAT	BRWDBAR_CNAT_002	H	H	H	H	H	H	H	H	H	H	H	H
CNAT	BRWDBAR_CNAT_004	H	H	H	H	H	H	H	H	H	H	H	H
CNAT	CN25_01 (former a&b)	H	H	H	H	H	H	H	H	H	H	U	U
CNAT	CN25_01 (former c&d)	H	H	H	H	H	H	O	O	O	O	O	O
CNAT	CN25_02 (former a&b)	H	H	H	H	H	H	H	H	H	H	H	H
CNAT	CN25_02 (former c&d)	H	H	H	H	H	H	O	O	O	O	O	O
CNAT	CN25_02e	H	H	H	H	H	H	O	O	O	O	O	O
CNAT	CN23_01R	H	H	H	H	H	H	H	H	H	H	H	H
CNAT	3_CNAT_003								N	H	H	H	H
CNAT	37_CNAT_001								N	H	H	H	H
CNAT	38_CNAT_005								N	H	H	H	H
DLAB	DL24_01	H	H	H	H	H	H	H	H	H	H	H	H
DLAB	DL20_01R	H	H	H	H	H	H	H	H	H	H	U	U
DLAB	DLX_01	H	H	H	H	H	H	H	H	H	H	H	H
DLAB	DLX_02	H	H	H	H	H	H	H	H	H	H	H	H
DLAB	DL24_01R	H	H	H	H	H	H	H	H	H	H	H	H
DLAB	DL24_02R	H	H	H	H	H	H	H	H	H	H	H	H
DLAB	DL25_01	H	H	H	H	H	H	H	U	D	D	D	D
DLAB	DL25_02	H	H	H	H	H	H	H	H	H	H	H	H
DLAB	DL25_03	H	H	H	H	H	H	H	H	H	H	H	H

Species	Coral ID	Jul	Aug	Sept	Oct	Nov	Dec	Jan	Feb	Mar	Apr	May	Jun
DLAB	DL25_04	H	H	H	H	H	H	H	H	H	U	H	U
DLAB	DL25_05	H	H	H	H	H	H	H	H	H	H	H	H
DLAB	DL25_06	H	H	H	H	H	H	U	U	H	H	H	H
DLAB	DL25_07	H	H	H	H	H	H	H	H	H	H	H	H
DLAB	DL25_08	H	H	H	H	H	H	H	H	H	H	H	H
DLAB	DL25_09	H	H	H	H	H	H	H	H	H	H	H	H
DLAB	DL25_10	H	H	H	H	H	H	H	H	H	H	H	H
DLAB	DL25_11	H	H	H	H	H	H	U	U	H	H	H	H
DLAB	3_DLAB_001								N	H	H	H	H
DLAB	38_DLAB_002								N	H	H	H	H
DLAB	39_DLAB_005								N	H	H	H	H
MCAV	MC_299_3	H	H	H	H	H	H	H	H	H	H	H	H
MCAV	MCX_01	H	H	H	H	H	H	H	H	H	H	H	H
MCAV	MCX_03	H	H	H	H	H	H	H	H	H	H	H	H
MCAV	MC19_01	H	H	U	U	H	H	H	H	H	H	H	H
MCAV	MC19_04	H	H	U	U	H	H	H	H	H	H	H	H
MCAV	MC19_18a	H	U	U	U	H	H	H	H	H	H	H	H
MCAV	MC19_18b	H	U	U	U	U	U	U	H	H	H	H	H
MCAV	MC19_21	H	H	H	H	H	H	H	H	H	H	H	H
MCAV	MC19_23a	H	H	H	H	H	H	H	H	H	H	H	H

Species	Coral ID	Jul	Aug	Sept	Oct	Nov	Dec	Jan	Feb	Mar	Apr	May	Jun
MCAV	MC19_23b	H	U	U	U	H	H	H	H	H	H	H	H
MCAV	MC19_31b	H	U	U	U	H	H	H	H	H	H	H	H
MCAV	MC19_34	H	H	H	U	H	H	H	H	H	H	H	H
MCAV	MC20_01	U	H	H	H	H	H	H	H	H	H	H	H
MCAV	MC20_02	U	U	U	U	H	H	H	H	H	H	H	H
MCAV	MC24_01	H	H	H	U	U	H	U	U	H	H	H	H
MCAV	MC24_02	H	H	H	H	H	H	H	H	H	H	H	H
MCAV	MC24_03	U	U	U	U	U	U	U	D	D	D	D	D
MCAV	MC24_04	H	H	H	H	H	H	H	H	H	H	H	H
MCAV	MC25_01	H	H	H	H	H	H	H	H	H	H	H	H
MCAV	BRWD277_MCAV_001	H	H	H	H	H	H	H	H	H	H	H	H
MCAV	BRWDBAR_MCAV_01	U	H	H	H	H	H	H	H	H	H	H	H
MCAV	BRWDBAR_MCAV_03	H	U	U	U	U	H	H	H	H	H	H	H
MCAV	BRWDBC1_MCAV_01	H	H	H	H	H	H	H	H	H	H	H	H
MCAV	BRWDBC2_MCAV_02	H	H	U	U	H	H	H	H	H	H	H	H
MCAV	BRWDCAVE_MCAV_02	H	H	H	U	H	H	H	H	H	H	H	H
MCAV	BRWDCAVE_MCAV_03	H	H	H	H	H	H	H	H	H	H	H	H
MCAV	BRWDCOM_MCAV_01	H	U	U	U	U	U	U	H	H	H	H	H
MCAV	BRWDJUL_MCAV_02	H	H	H	H	H	H	H	H	H	H	H	H
MCAV	BRWDJUL_MCAV_004a	U	H	H	H	H	H	H	H	H	H	H	H

Species	Coral ID	Jul	Aug	Sept	Oct	Nov	Dec	Jan	Feb	Mar	Apr	May	Jun
MCAV	39_MCAV_037								N	H	H	U	H
OFAV	OF20_01	H	H	H	H	H	H	H	H	H	H	H	H
OFAV	BRWDBAR_OFAV_001	H	H	H	H	H	H	H	H	H	H	H	H
OFAV	BRWDBAR_OFAV_005a	H	H	H	H	H	H	H	H	H	H	H	H
OFAV	BRWDBAR_OFAV_005b	H	H	H	H	H	H	H	H	H	H	H	H
OFAV	BRWDBAR_OFAV_005c	H	H	H	H	H	H	H	H	H	H	H	H
OFAV	BRWDBC1_OFAV_003a	H	H	H	H	H	H	H	H	H	H	H	H
OFAV	BRWDBC1_OFAV_003b	H	H	H	H	H	H	H	H	H	H	H	H
OFAV	BRWDBC2_OFAV_001	H	H	H	H	H	H	H	H	H	H	H	H
OFAV	BRWDBOU_OFAV_003	H	H	H	H	H	H	H	H	H	H	H	H
OFAV	BRWDJUL_OFAV_001	H	H	H	H	H	H	H	H	H	H	H	H
PCLI	PC21_01a	H	H	H	H	H	H	H	H	H	H	H	H
PCLI	PC21_01b	H	H	H	H	H	H	H	H	H	H	H	H
PCLI	PC21_02a	H	H	H	H	H	H	H	H	H	H	H	H
PCLI	PC21_02b	H	H	H	H	H	H	O	O	O	O	O	O
PCLI	PC24_01	H	H	H	H	H	H	H	H	H	H	H	H
PCLI	BRWD277_PCLI_002	H	H	H	H	H	H	H	H	H	H	H	H
PCLI	BRWD277_PCLI_003	H	H	H	H	H	H	H	H	H	H	H	H
PCLI	BRWD277_PCLI_004	H	H	H	H	H	H	H	H	H	H	H	H
PCLI	BRWD277_PCLI_005	H	H	H	H	H	H	H	H	H	H	H	H

Species	Coral ID	Jul	Aug	Sept	Oct	Nov	Dec	Jan	Feb	Mar	Apr	May	Jun
PCLI	BRWD277_PCLI_006a	H	H	H	H	H	H	H	H	H	H	H	H
PCLI	BRWD277_PCLI_007	H	H	H	H	H	H	H	H	H	U	U	H
PCLI	BRWD277_PCLI_008	H	H	H	H	H	H	H	H	H	H	H	H
PCLI	BRWD277_PCLI_010	H	H	H	H	H	H	H	U	U	U	U	U
PCLI	BRWD277_PCLI_011	H	H	H	H	H	H	H	H	H	H	H	H
PCLI	BRWD277_PCLI_012a	H	H	H	H	H	H	H	H	H	H	H	H
PCLI	BRWD277_PCLI_012c	H	H	H	H	H	H	H	H	H	H	U	U
PCLI	BRWD277_PCLI_015	H	H	H	H	H	H	H	H	H	H	H	H
PCLI	BRWDBAR_PCLI_002	H	H	H	H	H	H	H	H	H	H	H	H
PCLI	BRWDCOM_PCLI_001	H	H	H	H	H	H	H	U	U	U	U	U
PSTR	PS24_01	H	H	U	U	D	D	D	D	D	D	D	D
PSTR	BRWDBAR_PSTR_009	H	H	H	H	H	H	H	H	U	U	U	U
PSTR	BRWDJUL_PSTR_001	H	H	H	H	H	H	H	H	H	H	H	H
PSTR	PS25_01a (former a&b)	H	H	U	U	D	D	D	D	D	D	D	D
PSTR	PS25_02	H	H	H	H	H	H	H	H	H	H	H	H
PSTR	PS25_03a	H	H	H	H	H	H	H	H	H	U	U	D
PSTR	PS25_03b	H	H	H	D	D	D	D	D	D	D	D	D
PSTR	PS25_03c	H	H	H	D	D	D	D	D	D	D	D	D
PSTR	PS25_04	H	H	H	H	U	H	U	U	H	H	H	H
PSTR	PS25_05	H	H	H	U	D	D	D	D	D	D	D	D

Species	Coral ID	Jul	Aug	Sept	Oct	Nov	Dec	Jan	Feb	Mar	Apr	May	Jun
PSTR	PS25_06	H	H	H	U	U	U	U	U	U	U	U	U
PSTR	PS25_07	H	H	H	U	D	D	D	D	D	D	D	D
PSTR	PS25_08	H	H	H	H	H	H	H	H	H	H	H	H
PSTR	PS25_09	H	H	H	U	U	D	D	D	D	D	D	D
PSTR	PS25_10a (former a,b&c)	H	H	H	H	H	H	H	H	H	H	H	U
PSTR	PS25_11	H	H	D	D	D	D	D	D	D	D	D	D
PSTR	37_PSTR_001								N	H	H	H	H
PSTR	37_PSTR_003								N	H	H	H	H
SSID	SSX_001	H	H	H	H	H	H	O	O	O	O	O	O
SSID	SSX_002	H	H	H	H	H	H	O	O	O	O	O	O
SSID	SSX_003	H	H	H	H	H	H	H	H	H	H	H	H
SSID	SSX_004	H	H	H	H	H	H	H	H	H	H	H	H
SSID	SSX_005	H	H	H	H	H	H	H	H	H	H	H	H
SSID	SSX_006	H	H	H	H	H	H	H	H	H	H	H	H
SSID	SSX_007	H	H	H	H	H	H	O	O	O	O	O	O
SSID	SSX_008	H	H	H	H	H	H	O	O	O	O	O	O
SSID	SSX_009	H	H	H	H	H	H	O	O	O	O	O	O
SSID	SSX_010	H	H	H	H	H	H	H	H	H	H	H	H
SSID	SSX_011	H	H	H	H	H	H	O	O	O	O	O	O
SSID	SSX_012	H	H	H	H	H	H	O	O	O	O	O	O

Species	Coral ID	Jul	Aug	Sept	Oct	Nov	Dec	Jan	Feb	Mar	Apr	May	Jun
SSID	SSX_013	H	H	H	H	H	H	O	O	O	O	O	O
SSID	SSX_014	H	H	H	H	H	H	O	O	O	O	O	O
SSID	SSX_015	H	H	H	H	H	H	O	O	O	O	O	O

Water quality was maintained over time via biological, mechanical and chemical filtration, water changes, and phosphate and carbon reactors. Target levels were 140-160 ppm alkalinity, 420-450 ppm calcium, 1400-1500 ppm magnesium, 2-4 ppm nitrate, 0.001-0.005 ppm nitrite, 0.4-0.5 ppm phosphate, and 0 ppm ammonia. Magnesium was tested monthly; all other tests were run weekly. Temperature and salinity were measured and recorded daily. Throughout the year, the water samples matched the targeted values.

Fig 4. Broodstock *P. clivosa* colony in July 2025 and June 2026.

Fig 5. Broodstock *D. labyrinthiformis* colony in July 2025 and June 2026.

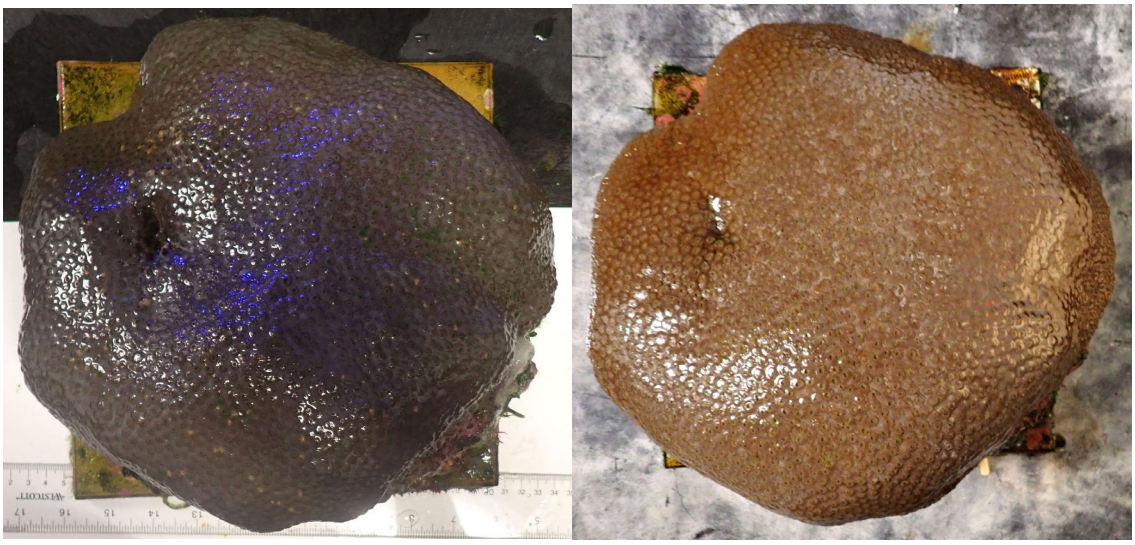

Fig 6. Broodstock *O. faveolata* colony in July 2025 and June 2026.

Fig 7. Broodstock *M. cavernosa* colony in July 2025 and June 2026.

- **Task 6: Grow-out of coral juveniles at the offshore nursery (Gilliam)**

Over 260 sexual recruits of *C. natans*, *D. laybrinthiformis*, *O. faveolata*, *M. cavernosa*, *P. clivosa* and *P. strigosa* (Table 3) were transferred to the NSU offshore nursery between January and February 2026. Based on the successful results of the previous year's mesh PED trials, PED tables were again used for all individuals for the duration of their offshore nursery phase. For all species except *D. labyrinthiformis* and *O. faveolata*, survival was 100% after 3 months (Table 3). The smaller mean deployment size (0.5 cm) of *D. labyrinthiformis* (Figure 8) likely reduced survivorship, while the low sample size combined with high algal overgrowth competition likely limited *O. faveolata* survival. In April 2026, an additional cohort of 296 *C. natans*, *M. cavernosa*, *P. clivosa*, and *P. strigosa* recruits were transferred to the offshore nursery using the same methodology. Survival for all species after 1 month was 100% (Table 4).

Table 3. Nursery survivorship from 1 week to 3 months for all species.

Group ID	Species	# Deployed	Mean Deployment Size (cm)	1 week Survivorship	1 month Survivorship	3 months Survivorship
2026 Cohort 1	CNAT	102	2.5 ± 0.05	100%	100%	100%
2026 Cohort 1	DLAB	27	0.5 ± 0.04	89%	85%	67%
2026 Cohort 1	MCAV	51	1.7 ± 0.08	100%	100%	100%
2026 Cohort 1	OFAV	6	2.7 ± 0.22	100%	100%	33%
2026 Cohort 1	PCLI	40	4.0 ± 0.68	100%	100%	100%
2026 Cohort 1	PSTR	40	2.6 ± 0.08	100%	100%	100%
2026 Cohort 2	CNAT	121	3.2 ± 0.07	100%	100%	NA
2026 Cohort 2	MCAV	60	1.9 ± 0.20	100%	100%	NA
2026 Cohort 2	PCLI	55	3.4 ± 0.20	100%	100%	NA
2026 Cohort 2	PSTR	60	3.6 ± 0.15	100%	100%	NA

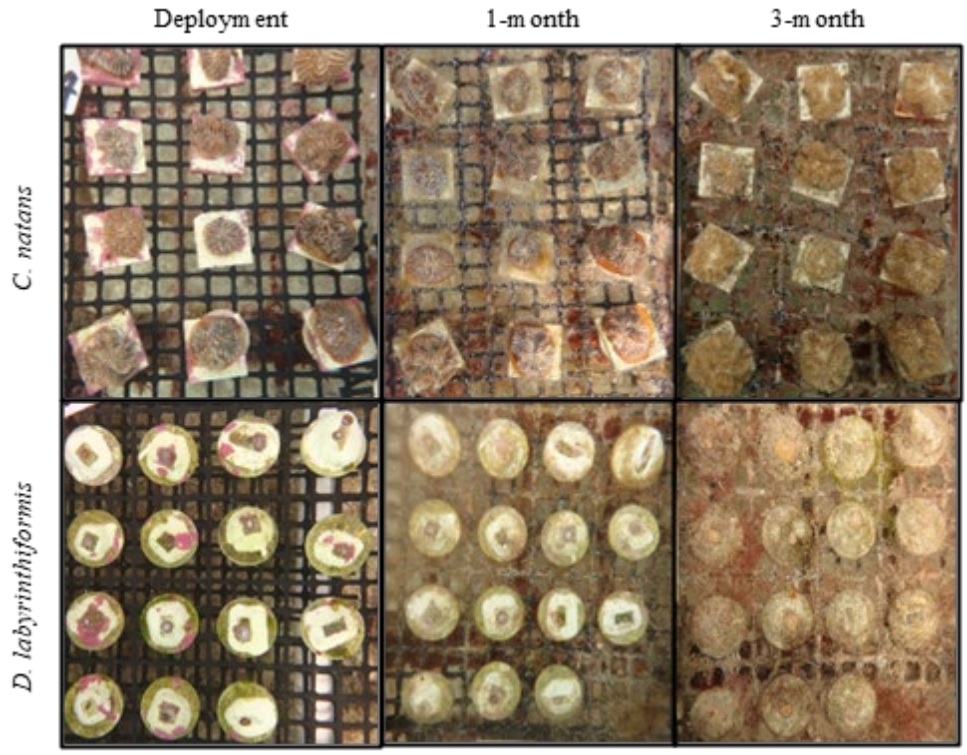

Fig 8. Time series monitoring images (deployment, 1-month, 3-month) of *C. natans* and *D. labyrinthiformis* recruits transferred to NSU's offshore PED mesh table.

Additionally, during January 2026, a subset of *C. natans*, *M. cavernosa*, *P. clivosa*, and *P. strigosa* recruits were outplanted to a site on the inner reef in southern Broward County (South Spawning Hub: C9-1, C9-2) and all corals were caged with a mesh PED (Figure 9). Survivorship at 3 months was high for all species (Table 4).

Fig 9. A *P. clivosa* recruit outplanted with a mesh PED at the South Spawning Hub.

Table 4. Outplant survivorship: 1 week - 3 months for all species.

Group ID	Species	# Deployed	1 week Survivorship	1 month Survivorship	3 months Survivorship
2026 Cohort 1	CNAT	40	100%	100%	100%
2026 Cohort 1	MCAV	40	100%	98%	95%
2026 Cohort 1	PCLI	40	100%	100%	95%
2026 Cohort 1	PSTR	40	100%	100%	100%

Lastly, between October 2024 and May 2026, monitoring of corals outplanted during previous years (2021-2025) was conducted, which included colony condition and planar images. Mean survival across all sites and all species for each outplant year was as follows: 2021 = 3%, 2022 = 50%, 2023 = 50%, 2024 = NA, 2025 = 76% (see supplemental document “Task 6_Nursery and Outplant Survival Summary”).

- **Task 7: Settlement trials with CYPRO (Figueiredo & Schupp)**

- Well plate experiments

Diploria labyrinthiformis larvae were observed to accumulate CYPRO (Figure 10-A), similarly to what has previously been observed with larvae of other coral species (Fiegel et al., 2025) and settled in a concentration-dependent manner (Figure 10). Settlement was most successful using the total amount of 1 µg per well where a proportion of 14.2 – 42.9% of the larvae settled.

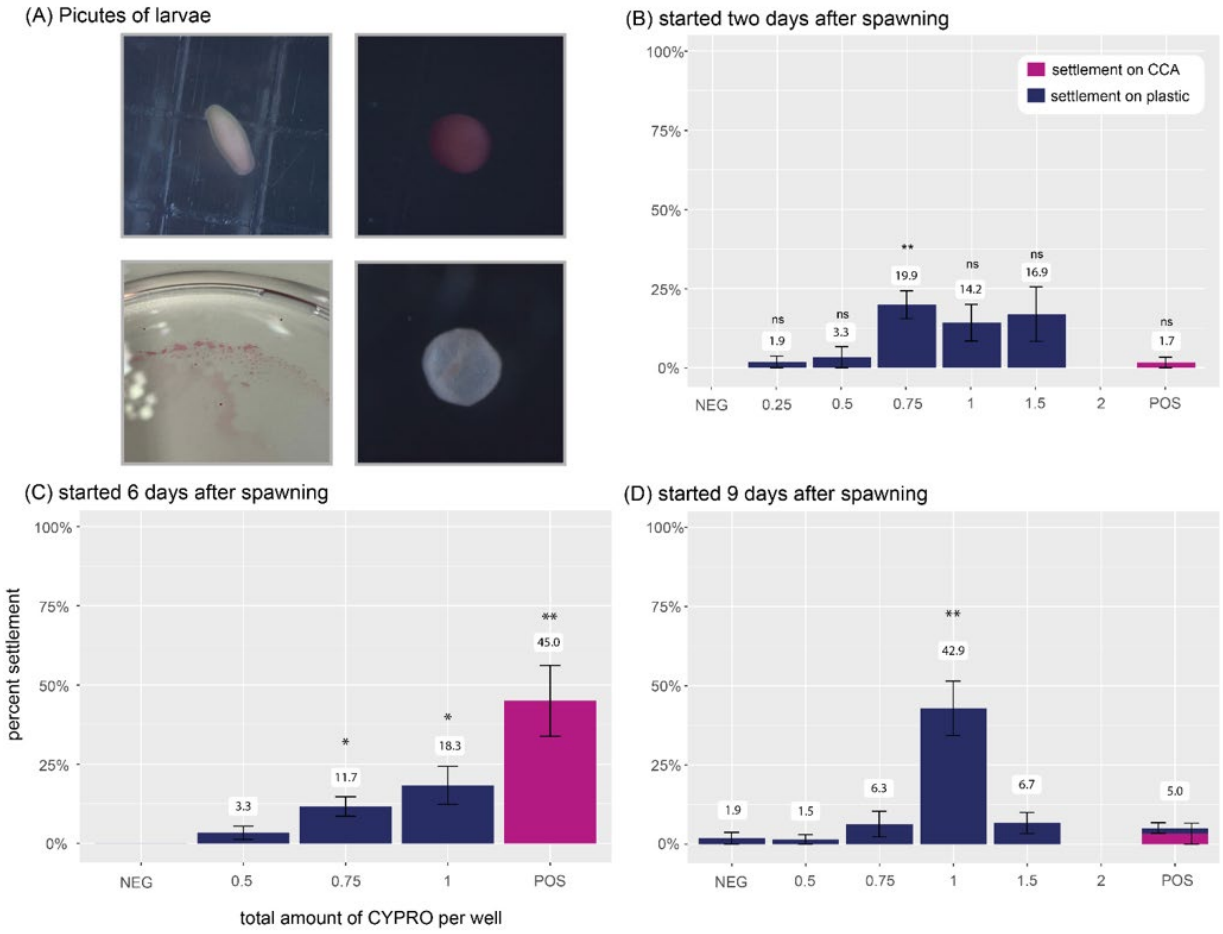

Fig 10. (A) Pictures of top left - swimming larvae, top right - larvae after accumulating CYPRO, bottom left - larvae swimming over the CYPRO film on the bottom of the well, bottom right – settled recruit. (B) – (D) Mean proportion of D. labyrinthiformis larvae settled, exposed to CYPRO, across different concentrations. NEG – negative control, POS – CCA positive control. The same experiment was conducted three times, 2, 6, and 9 days after spawning. Statistical

significance was tested pairwise against the control treatment. The error bar displays standard error (SE).

Settlement in the CCA positive control was highly variable with a proportion of 1.7 – 45% of the larvae settled. This indicates that CCA alone is not always a reliable settlement inducer.

- PRIMING experiments

The PRIMING experiments were conducted to test if the larvae can be transferred to a second container after they have accumulated the settlement cue. This method would allow for the development of exposure methods that are more saleable and suitable for restoration purposes. Two experiments were conducted (A) CYPRO exposure for 10 hours and (B) CYPRO exposure for 11 hours in a range of concentrations. Larvae settled with highest success when exposed to 6 µg per petri dish with 24.4 % and 38.2 % (Figure 11). However, after 11 hours of pre-exposure, a high proportion of the larvae settled already before the transfer to the second container across all applied concentrations.

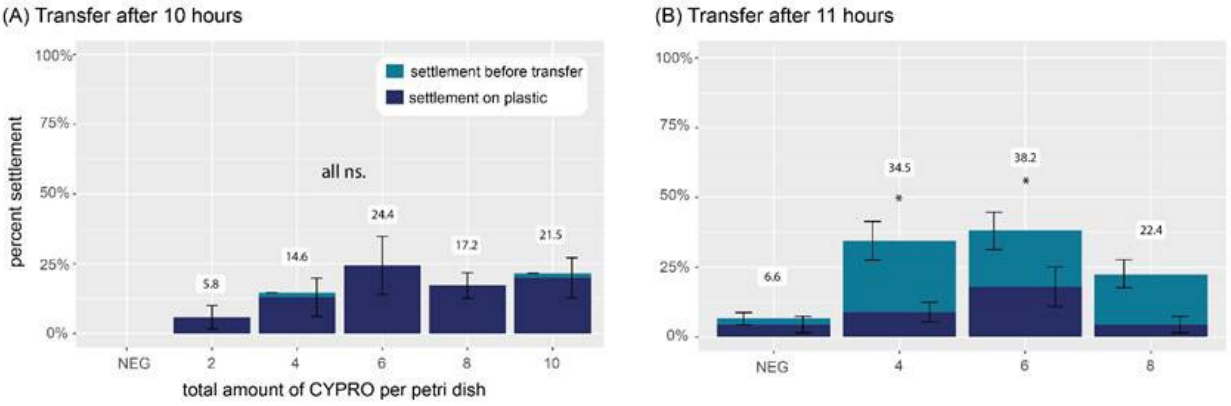

Fig 11. The mean proportion of *D. labyrinthiformis* settled after (A) 10 hours and (B) 11 hours of CYPRO pre-exposure. Statistical significance was tested pairwise against the control treatment. The error bar displays standard error (SE).

- **Task 8: Genome-wide parentage analysis and thermal stress response of parental colonies (Gomez-Corrales and Liberman)**

- Broodstock Tissue Collection and DNA/RNA Extraction

Tissue samples were collected from 13 *M. cavernosa* broodstock colonies maintained at NSU's land-based nursery. All colonies originated from KJCAP and are survivors of the (SCTLD outbreak, representing 11 unique genotypes (two genotypes, MC19_18 and MC19_23, each contributed two fragments). Tissue biopsies were collected on February 25, 2026, and preserved in RNA/DNA Shield (Zymo Research) for downstream nucleic acid extraction.

Tissue homogenization was performed on March 20, 2026, and DNA extractions were completed on March 23 and March 30, 2026, using a Zymo Quick-DNA/RNA Miniprep Plus kit (Cat. no. D7003) (50 µl elution volume per analyte; 8 µl aliquoted for quality control). DNA quantity was assessed by Qubit fluorometry and quality by agarose gel (1%) electrophoresis. All 13 samples yielded high-molecular-weight DNA suitable for whole-genome sequencing (Table 5). To ensure the highest DNA quality, extractions were cleaned using the Genomic DNA Clean & Concentrator-10 kit (Zymo Research, Cat. no. D4011). Samples were submitted to the University of Florida ICBR Gene Expression and Genotyping Core (Gainesville, FL) for library preparation and WGS. Libraries were prepared in June 2026, and samples were queued for sequencing on an Illumina NovaSeq X (10B, 2×150 bp; ~375 Gb output per lane) in July 2026. This data will support parentage analysis and estimation of effective population size across the broodstock cohort.

Table 5. Summary of tissue collection, nucleic acid extraction, and cp23S sequencing from *M. cavernosa* broodstock colonies. All samples collected on February 25, 2026, and preserved in RNA/DNA Shield. DNA quality assessed by gel electrophoresis and DNA quantity was measured on a Qubit fluorometer; HMW = high-molecular-weight DNA.

Colony ID	Unique Genotype	Qubit DNA (ng/µl)	Gel Quality	Algal Symbiont Genus
MC19_01	MC19_01	>100*	HMW	*Cladocopium (C)*
MC19_04	MC19_04	>100*	HMW	NA
MC19_10	MC19_10	>100*	HMW	*Cladocopium (C)*
MC19_18A	MC19_18	>100*	HMW	*Cladocopium (C)*
MC19_18B	MC19_18	>100*	HMW	*Cladocopium (C)*
MC20_01	MC20_01	>100*	HMW	*Cladocopium (C)*
MC19_23A	MC19_23	>100*	HMW	*Cladocopium (C)*
MC19_23B	MC19_23	>100*	HMW	*Cladocopium (C)*
MC19_29	MC19_29	>100*	HMW	*Cladocopium (C)*
MC19_31B	MC19_31B	>100*	Low-HMW	*Cladocopium (C)*
MC19_34	MC19_34	104	Low-HMW	*Cladocopium (C)*
MC24_01	MC24_01	>100*	HMW	*Cladocopium (C)*
MC24_02	MC24_02	76.6	Low-HMW	*Durusdinium (D)*

**Qubit readings exceeded the upper limit of the assay standard range. – indicates RNA yield below quantification threshold.*

- Algal Symbiont Identification via cp23S Sequencing

Algal symbiont genotyping was performed on all 13 broodstock colonies and all nine CBASS juveniles by PCR amplification and Sanger sequencing of the chloroplast 23S ribosomal RNA gene (cp23S) with primers 23S1M13/23S2M13 (Zhang et al., 2000). Amplicons were verified by gel electrophoresis prior to sequencing. Among the broodstock, 12 of 13 colonies returned usable

cp23S sequences; one sample (MC19_04) failed to yield a clean sequence. To identify the dominant symbiont genus in each colony, the cp23S sequences were aligned together with GenBank reference sequences spanning Cladocopium and *Durusdinium* genera (family = Symbiodiniaceae), and a maximum-likelihood phylogenetic tree was constructed (Figure 17).

The analysis resolved a clear separation between two symbiont genera: *Cladocopium* (clade C) and *Durusdinium* (clade D). Eleven of the twelve sequenced broodstock colonies hosted *Cladocopium*, the symbiont genus most commonly associated with *M. cavernosa* on Florida's Coral Reef. A single broodstock colony, MC24_02, hosted *Durusdinium*, a genus generally associated with elevated thermal tolerance. In contrast, all nine CBASS juveniles hosted *Durusdinium* (see CBASS section below), indicating a marked difference in symbiont association between the broodstock and the nursery-reared juveniles.

- CBASS Thermal Stress Experiment

An acute short-term CBASS thermal stress assay was conducted on May 12, 2026, targeting nine *M. cavernosa* over one-year-old juveniles produced during the 2024 spawning season. Colonies were assigned to three thermal treatments (n = 3 per treatment) using stratified randomization based on pre-experiment baseline Fv/Fm values to ensure balanced photosynthetic starting conditions across groups: Control (ambient, 26°C), moderate heat (CBASS-1, target 29°C; +3°C above ambient), and severe heat (CBASS-2, target 32°C; +6°C above ambient). Three tanks were operated in parallel at NSU's marine science facility.

The experimental timeline comprised five phases: baseline monitoring (20:00 May 11 – 12:00 May 12), ramp-up (12:00–15:00; 3-hour linear ramp to target temperature), hold (15:00–18:00; 3 hours at target temperature), cool-down (18:00–19:00), and overnight recovery (19:00 May 12 – 08:00 May 13). Temperature was continuously logged using two independent sensor systems: HOBO MX2202 pendant loggers (Onset Computer Corporation; ±0.2°C accuracy; 2-min intervals, resampled to 10-min means) and an Apex A3 aquaculture controller probe (Neptune Systems;

±0.1°C accuracy; 10-min intervals). CBASS-1 and CBASS-2 each carried paired HOBO loggers (A and B) positioned at opposite ends of the tank to capture any spatial temperature variation; the Control tank carried a single HOBO logger.

Target temperatures were delivered with high fidelity across all phases (Table 6; Figures 12–14). During the hold window (15:00–18:00 EDT), mean temperatures across all sensors were 29.05°C ±0.95°C for CBASS-1 (target 29°C; deviation +0.02°C), 32.29°C ±0.194°C for CBASS-2 (target 32°C; deviation +0.25°C), and 26.08°C ±0.13°C for the Control (target 26°C). Warming rates during the ramp phase were 0.85°C/hr for CBASS-1 and 1.85°C/hr for CBASS-2, consistent with their respective linear ramp profiles. Following the hold window, both treatment tanks cooled rapidly: CBASS-1 returned to ≤26°C at 18:40 EDT (cool-down rate 2.62°C/hr) and CBASS-2 at 19:10 EDT (5.47°C/hr). A brief temperature undershoot below ambient was detected in CBASS-2 during the overnight period — a characteristic feature of CBASS systems operating at large temperature differentials — but all three tanks had stabilized at equivalent near-ambient conditions by the overnight recovery period (Control 25.97°C ±0.09°C, CBASS-1 26.05°C ±0.17°C, CBASS-2 26.18°C ±0.17°C), ensuring that differences in photosynthetic recovery on May 13 reflect thermal history during the experiment rather than ongoing temperature differences at the time of measurement. Inter-sensor agreement was strong: paired HOBO loggers within CBASS-2 differed by a mean of only 0.039°C during the hold window, confirming thermal homogeneity within that tank; the 0.415°C difference observed within CBASS-1 reflects a documented spatial temperature gradient rather than a calibration artifact.

Table 6. Phase-level temperature statistics (mean ± SD, min, max) across all sensors combined (HOBO-A, HOBO-B where available, and Apex probe) for five experimental phases. Baseline: 20:00 May 11 – 12:00 May 12; Ramp-up: 12:00–15:00; Hold: 15:00–18:00; Cool-down: 18:00–19:00; Overnight: 19:00 May 12 – 08:00 May 13. The Control tank was monitored with HOBO-A and Apex only (no HOBO-B deployed). The Ramp-up phase is not applicable to the Control tank, which was held constant at 26°C throughout.

Tank	Phase	Mean (°C)	SD (°C)	Min (°C)	Max (°C)
Control	Baseline	26.11	0.177	25.80	26.49
Control	Ramp-up	26.04	0.141	25.80	26.19
Control	Hold	26.09	0.126	25.80	26.22
Control	Cool-down	26.07	0.063	25.90	26.14
Control	Overnight	25.97	0.091	25.80	26.20
CBASS-1 (29°C)	Baseline	26.19	0.184	25.80	26.54
CBASS-1 (29°C)	Ramp-up	27.79	0.786	26.30	29.21
CBASS-1 (29°C)	Hold	29.05	0.195	28.80	29.37
CBASS-1 (29°C)	Cool-down	27.04	0.950	26.06	28.97
CBASS-1 (29°C)	Overnight	26.05	0.165	25.76	26.40
CBASS-2 (32°C)	Baseline	26.26	0.269	25.80	26.80
CBASS-2 (32°C)	Ramp-up	29.57	1.610	26.80	32.27
CBASS-2 (32°C)	Hold	32.29	0.194	31.80	32.49
CBASS-2 (32°C)	Cool-down	29.08	1.735	26.30	31.88
CBASS-2 (32°C)	Overnight	26.18	0.168	25.80	26.47

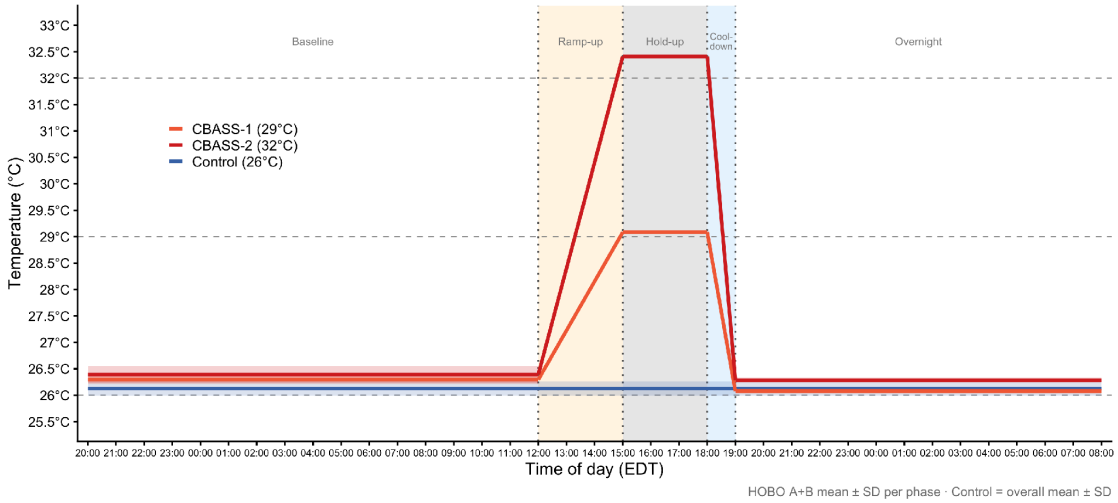

Fig 12. Full experimental timeline (HOBO A+B mean). Phase mean ± SD (shaded band) shown for constant-temperature periods: Baseline (20:00 May 11 – 12:00 May 12), Hold (15:00–18:00), and Overnight (19:00 May 12 – 08:00 May 13). Connecting lines span the Ramp-up and Cool-down transitions. Dashed horizontal lines at 26, 29, and 32°C indicate target temperatures. Dotted vertical line marks the time at which CBASS-2 returned to ≤26°C.

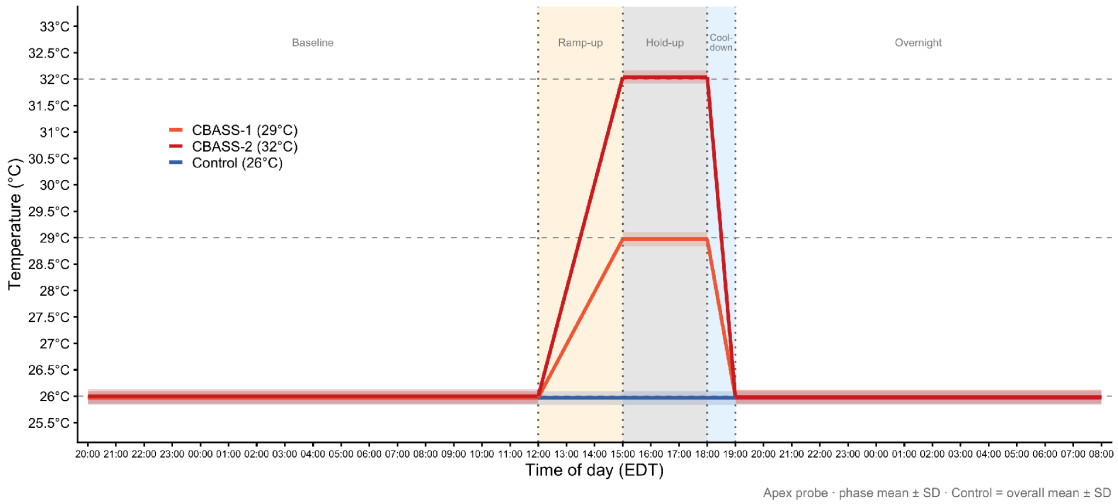

Fig 13. Full experimental timeline using Apex probe temperatures only. Phase structure and layout identical to Figure 12. Apex data provided an independent verification of the HOBO-derived temperature profile; connecting lines span the Ramp-up and Cool-down transitions between constant-temperature phases.

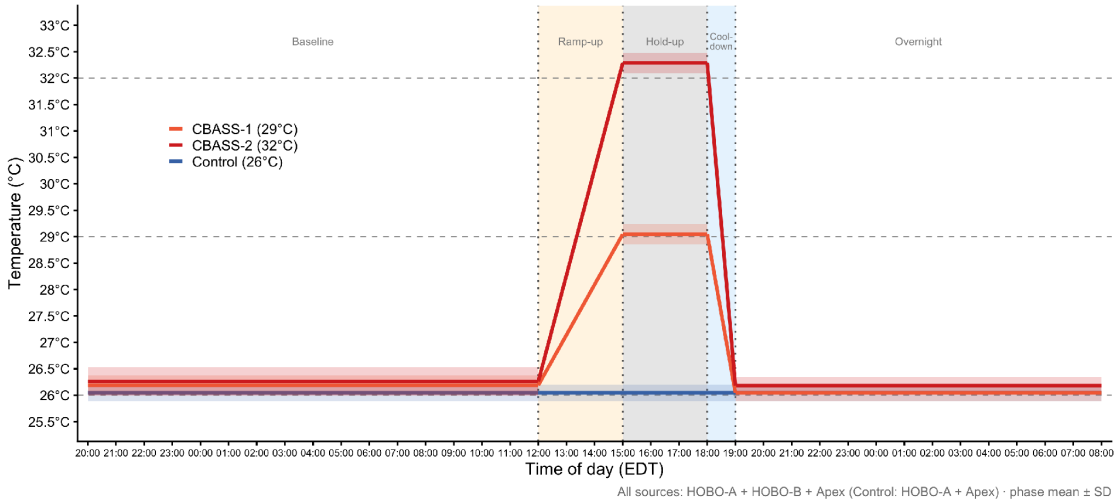

Fig 14. Full experimental timeline using all available temperature sources combined. For CBASS-1 and CBASS-2, mean ± SD is computed across HOBO-A, HOBO-B, and Apex probe per phase (three sensors). For the Control, mean ± SD reflects HOBO-A and Apex only (no HOBO-B deployed). SD captures both temporal variability within each phase and inter-sensor spread, providing the most conservative estimate of thermal treatment stability.

Photosynthetic Performance (Fv/Fm) Results

Photosynthetic efficiency (Fv/Fm) was measured using a Diving-PAM fluorometer (Walz) under dark-adapted conditions. Pre-experiment baseline measurements were collected across four dates (May 5, 6, 7, and 11, 2026), providing multiple readings per colony to characterize individual baseline variability; when multiple readings were collected on the same date, values were averaged to yield one daily mean per colony. Post-heat measurements were taken on May 12 immediately following thermal exposure and removal of colonies from the CBASS tanks. Recovery measurements were collected on May 13, after all tanks had returned overnight to equivalent near-ambient temperatures (25.97–26.18°C; Table 6), ensuring that Fv/Fm differences at recovery reflect thermal history rather than ongoing temperature differences. Treatment-level effects were assessed using a linear mixed-effects model ($Fv/Fm \sim Phase \times Treatment + (1|Colony)$) fitted with lmerTest in R, with pairwise comparisons via estimated marginal means (emmeans, Tukey-adjusted).

The linear mixed model revealed a highly significant effect of the experimental phase on Fv/Fm ($p < 0.001$), indicating that photosynthetic performance declined across all groups after heat exposure. However, there was no significant difference between treatments at the group level ($p = 0.668$), and the phase × treatment interaction was also not significant ($p = 0.575$). The overall decline likely reflects a combination of handling stress from transferring colonies into the CBASS system and the thermal exposure itself.

When comparing each treatment against its own baseline, only the +6°C group showed a statistically significant decline in Fv/Fm after heat exposure ($p = 0.006$, Tukey-adjusted). The Control and +3°C groups also declined but not significantly ($p = 0.387$ and $p = 0.243$, respectively), suggesting a dose-dependent thermal effect that becomes detectable at +6°C above ambient. The small sample size ($n = 3$ colonies per treatment) limits statistical power to resolve moderate treatment effects.

Per-colony analysis provided a clearer resolution of thermal effects. Five colonies in the +3°C and +6°C treatments showed significant post-heat declines in Fv/Fm ($p < 0.05$), while none of the three Control colonies declined significantly. This pattern is consistent with a real thermal effect superimposed on general handling stress. Recovery was variable among genotypes: in the +6°C group, Colonies 2 and 3 returned close to baseline levels while Colony 7 remained significantly depressed ($p = 0.007$). In the +3°C group, Colony 1 showed further decline during recovery ($p < 0.001$), warranting investigation in future assays. By the recovery measurement, all three groups converged to similar Fv/Fm values (~0.63), indicating that the Control decline was primarily a tank acclimation effect rather than lasting photosynthetic damage.

These results demonstrate that short-duration thermal stress at +6°C above ambient produces measurable and statistically significant declines in photosynthetic performance in *M. cavernosa* juveniles. Colony-level variation in recovery trajectory was substantial: some genotypes restored baseline Fv/Fm within 24 hours while others remained suppressed or continued to decline. This variation is directly relevant to broodstock and outplant candidate selection: genotypes that

maintain or rapidly recover Fv/Fm after thermal stress are better suited for restoration at sites subject to periodic heat events. Pairing these thermal-tolerance rankings with the WGS-based parentage assignments (Tables 5 and 7; Ongoing Analyses) will allow direct identification of which broodstock colonies produced thermally resilient offspring.

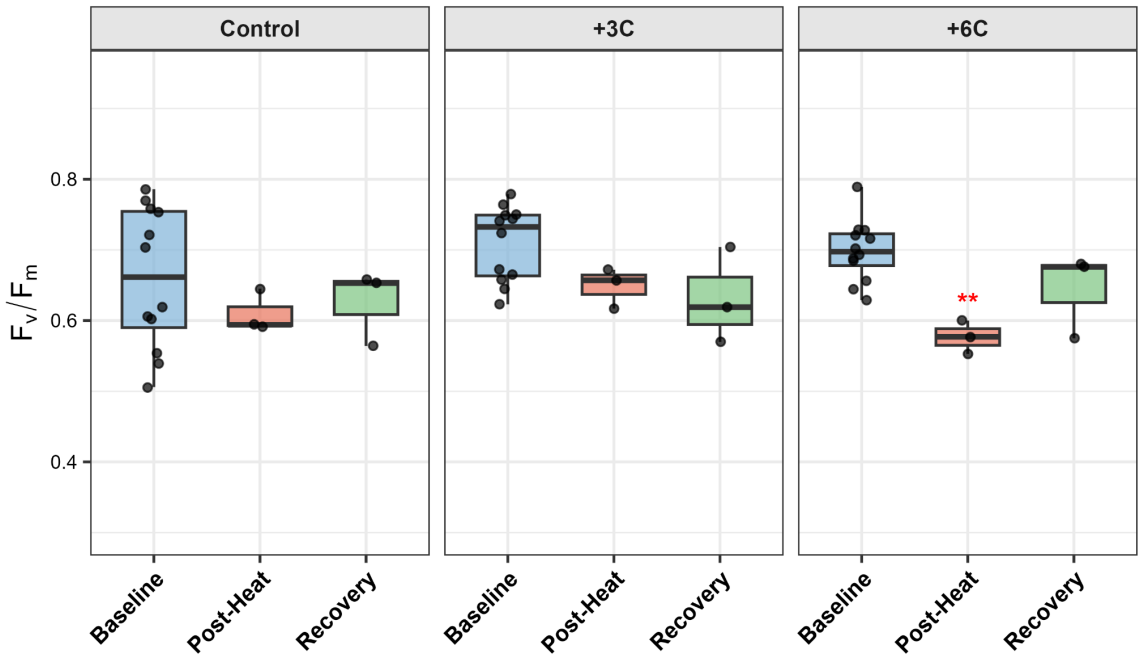

Fig 15. Fv/Fm by treatment across experimental phases (Baseline, Post-Heat, Recovery). Boxplots show the distribution of daily-averaged Fv/Fm values with individual data points overlaid. Significance annotations (** $p < 0.01$) indicate Tukey-adjusted pairwise comparisons against baseline. Only the +6°C treatment showed a statistically significant decline from baseline at the post-heat stage ($p = 0.006$).

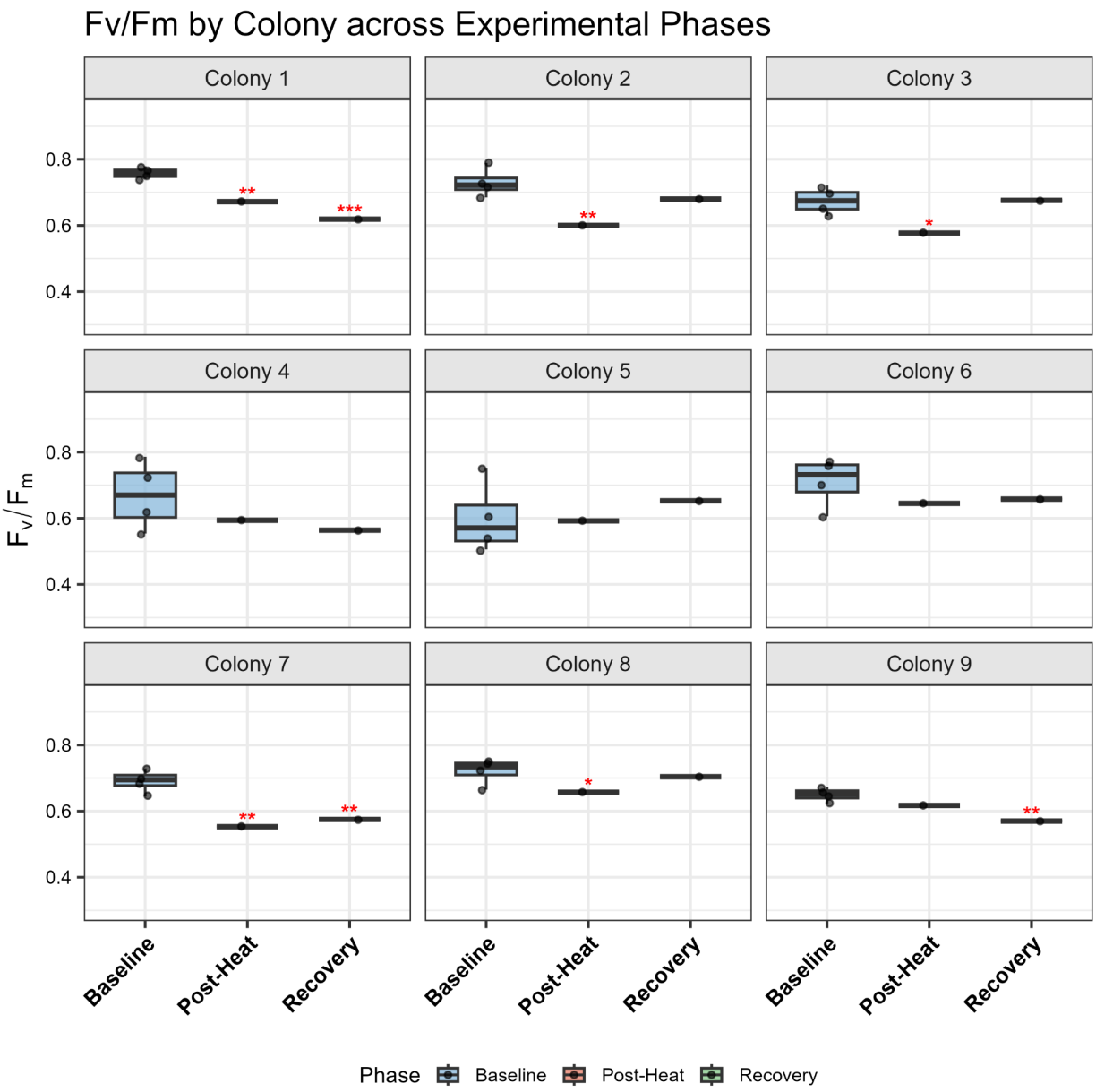

Fig 16. Fv/Fm by individual colony across experimental phases. Significance annotations (* $p < 0.05$, ** $p < 0.01$, *** $p < 0.001$) indicate one-sample t-tests comparing post-heat or recovery values against each colony's own baseline distribution. Control colonies (4, 5, 6) showed no significant changes, while all five of the six treated colonies showed significant post-heat declines. Recovery responses were genotype-dependent.

- CBASS Post-Experiment Tissue Preservation

Following the CBASS experiment, tissue samples were collected from all nine juvenile colonies on May 13, 2026. Each colony was sampled into one tube of RNA/DNA Shield for nucleic acid preservation, and an additional tissue fragment was wrapped in aluminum foil and stored at −80°C for downstream physiological analyses. Tissue was homogenized on May 19, 2026, and DNA extraction was completed on May 20, 2026. All samples yielded high-molecular-weight DNA (Table 7). Extractions were cleaned using the Genomic DNA Clean & Concentrator-10 kit (Zymo Research, Cat. no. D4011). These samples were submitted to the University of Florida ICBR Gene Expression and Genotyping Core alongside the broodstock extracts for library preparation and whole-genome sequencing on the same Illumina NovaSeq X run (July 2026). The combined sequencing dataset will enable parentage assignment of juveniles to broodstock genotypes and support genotype–thermal tolerance association analyses linking CBASS Fv/Fm responses to specific parental lineages.

Table 7. Tissue collection and DNA extraction summary for *M. cavernosa* juveniles following the CBASS thermal stress experiment. All samples were preserved in RNA/DNA Shield and stored at −80°C.

#	Colony ID	CBASS Tank	Temp (°C)	Collection Date	Homog. Date	Qubit DNA (ng/µl)	Gel Quality	Algal Symbiont Genus
18	1	CBASS-1	29	05/13/2026	05/19/2026	87.3	HMW	*Durusdinium (D)*
19	2	CBASS-2	32	05/13/2026	05/19/2026	73.0	HMW	*Durusdinium (D)*
20	3	CBASS-2	32	05/13/2026	05/19/2026	>100*	HMW	*Durusdinium (D)*
21	4	Control	26	05/13/2026	05/19/2026	>100*	HMW	*Durusdinium (D)*
22	5	Control	26	05/13/2026	05/19/2026	>100*	HMW	*Durusdinium (D)*
23	6	Control	26	05/13/2026	05/19/2026	>100*	HMW	*Durusdinium (D)*
24	7	CBASS-2	32	05/13/2026	05/19/2026	>100*	HMW	*Durusdinium (D)*
25	8	CBASS-1	29	05/13/2026	05/19/2026	>100*	HMW	*Durusdinium (D)*
26	9	CBASS-1	29	05/13/2026	05/19/2026	>100*	HMW	*Durusdinium (D)*

**Qubit readings exceeded the upper limit of the assay standard range.*

- Symbiont identity of CBASS juveniles

Algal symbiont genotyping (cp23S; see Algal Symbiont Identification above) showed that all nine juveniles used in the CBASS experiment hosted *Durusdinium* (clade D), in contrast to the broodstock, which were predominantly *Cladocopium* (clade C) (Figure 17). This uniform *Durusdinium* association most likely reflects symbiont uptake under nursery conditions rather than parental origin. *Durusdinium* is generally associated with greater thermal tolerance, which is relevant to interpreting the colony-level differences in photosynthetic recovery described above: because all juveniles shared the same symbiont genus, the variation in thermal response among them is more likely attributable to coral host genotype than to symbiont genus. Finer-resolution symbiont typing (ITS2 metabarcoding) planned for Year 2 will determine whether more subtle differences in symbiont community composition contribute to the observed variation in thermal performance.

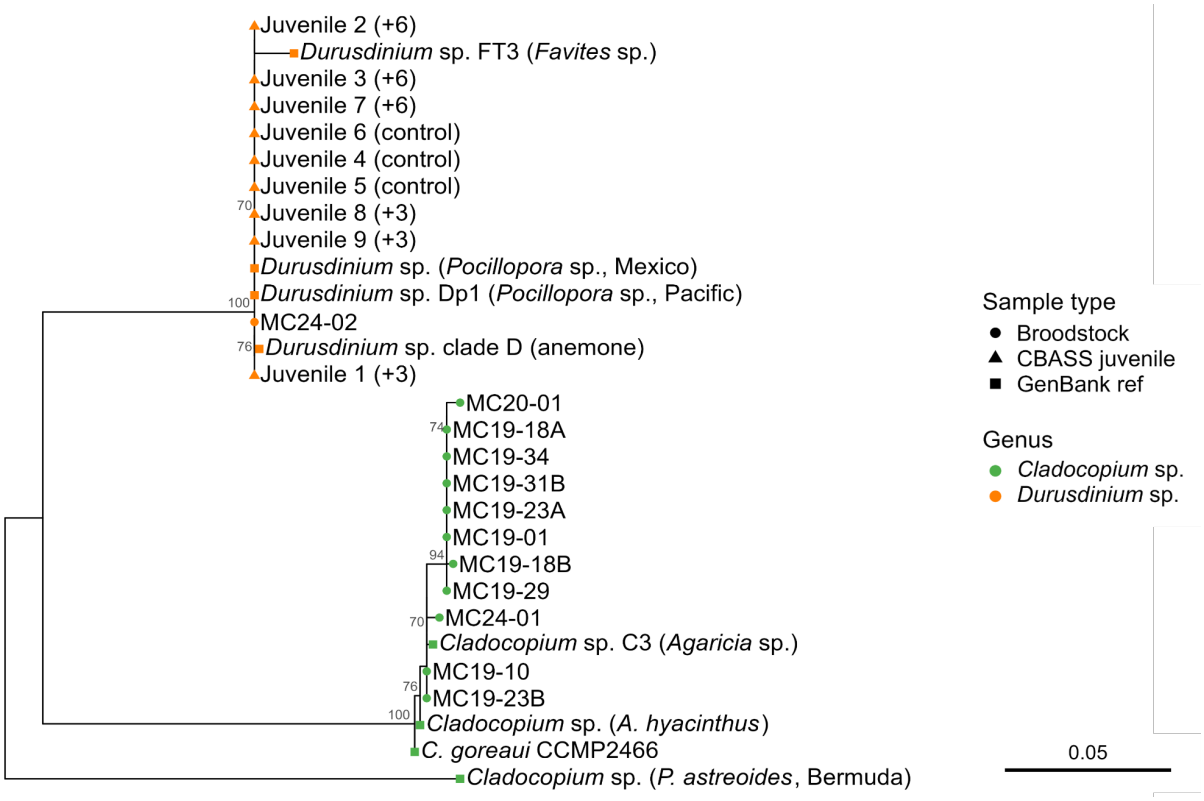

Fig 17. Maximum-likelihood phylogenetic tree of algal symbiont (Symbiodiniaceae) cp23S ribosomal RNA gene sequences from *M. cavernosa* broodstock colonies and CBASS-exposed

juveniles maintained at the NSU land-based nursery. The tree includes 29 sequences: 11 *Cladocopium* sp. (clade C) broodstock, one *Durusdinium* sp. (clade D) broodstock (MC24-02), nine juveniles hosting *Durusdinium* sp., and eight GenBank reference sequences for phylogenetic context. The two major clades correspond to the genera *Cladocopium* and *Durusdinium*, consistent with previous cp23S-based classifications. All broodstock colonies except MC24-02 harbored *Cladocopium* sp., while all CBASS juveniles harbored *Durusdinium* sp. Branch support values (≥70%) from ultrafast bootstrap analysis are shown at internal nodes. The tree was inferred using IQ-TREE with automatic model selection (best-fit model: HKY+F+I) and midpoint-rooted for display.

- **Task 9: Assessing energetics of coral early life stages and breeding stock to enhance nursery efficiencies (Martinez)**

- Metabolic rate through development

Oxygen-consumption rates increased with developmental time in field-derived larvae, and this pattern was evident at both temperatures (Figure 18). At 26°C, mean metabolic rates rose from 0.0191nmol O_2 $min^{-1}larva^{-1}$ at 20.5 hpf to 0.0354 at 43 hpf and reached 0.0624 O_2 $min^{-1}larva^{-1}$ by 66 hpf, though variability increased substantially at the latest stage (STDEV = 0.0921). Field larvae at 30°C showed a similar developmental trajectory, beginning at 0.0217 O_2 $min^{-1}larva^{-1}$ at 20.5 hpf and increasing to 0.0718 O_2 $min^{-1}larva^{-1}$ at 43 hpf before stabilizing near 0.0665 O_2 $min^{-1}larva^{-1}$ at 66 hpf. Across all matched time points, metabolic rates tended to be slightly higher at 30°C than at 26°C, suggesting a modest thermal increase of oxygen demand in field-sourced larvae.

The two-way ANOVA showed that developmental time of field larvae had a significant effect on oxygen-consumption rate ($F_{2,44} = 4.10$, $P = 0.023$), with metabolic rates increasing from 20.5 hpf to later stages. Holm–Sidak comparisons indicated that larvae at 66 hpf had significantly higher metabolic rates than those at 20.5 hpf, while the intermediate 43 hpf group did not differ significantly from either stage. In contrast, temperature did not significantly influence metabolic rate ($F_{1,44} = 1.29$, $P = 0.262$), and the interaction between developmental time and temperature was also non-significant ($F_{2,44} = 0.80$, $P = 0.457$), indicating that developmental increases in

metabolism occurred similarly at both 26°C and 30°C. Power analyses suggested moderate power for detecting developmental effects but low power for temperature and interaction terms. Least-squares means supported these patterns, with metabolic rates rising across developmental stages but showing only modest differences between temperatures.

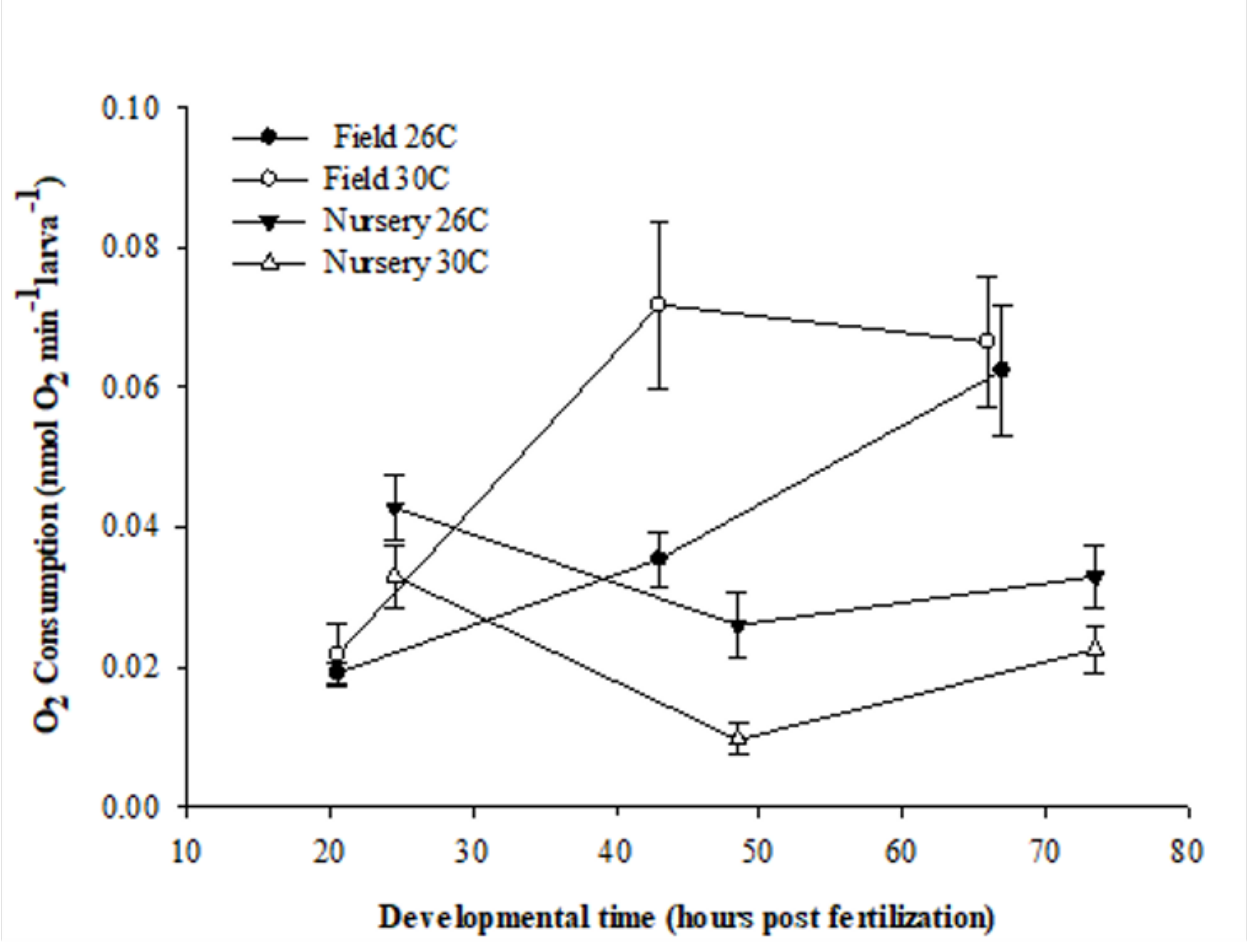

Fig 18. Aerobic metabolism of *D. labyrinthiformis* larva form field collected gametes (circles) and from nursery collected gametes (triangles) as a function of development time after fertilization. Mean ±SEM are shown (n=9).

Nursery-derived larvae displayed a different pattern, with metabolic rates generally lower and more variable across developmental stages and temperatures (Figure 18). At 26°C, oxygen consumption peaked early (0.0428 O_2 $min^{-1}larva^{-1}$ at 24.5 hpf) and then declined at 48.5 hpf (0.0260 O_2 $min^{-1}larva^{-1}$) before rising slightly by 73.5 hpf (0.0329). At 30°C, nursery larvae again

showed their highest rate at the earliest stage (0.0330 O_2 $min^{-1}larva^{-1}$ at 24.5 hpf), followed by a pronounced drop at 48.5 hpf (0.00955 O_2 $min^{-1}larva^{-1}$) and a partial rebound by 73.5 hpf (0.0225 O_2 $min^{-1}larva^{-1}$). Compared with field larvae, nursery larvae exhibited weaker developmental increases and greater fluctuations across time, indicating that source population and thermal environment jointly shape early metabolic trajectories.

Contrary to field derived larvae, the two-way ANOVA revealed strong effects of both developmental time and temperature on metabolic rate. Developmental time had a highly significant influence ($F_{2,48} = 11.96$, $P < 0.001$), with Holm–Sidak comparisons showing that all three stages differed from one another: metabolic rates were highest at 24.5 hpf, lowest at 48.5 hpf, and intermediate at 73.5 hpf. Temperature also significantly affected metabolic rate ($F_{1,48} = 13.31$, $P < 0.001$), with larvae at 26°C exhibiting higher mean rates (0.0339) than those at 30°C (0.0217). In contrast, the interaction between developmental time and temperature was not significant ($F_{2,48} = 0.41$, $P = 0.666$), indicating that the developmental pattern of metabolic change was similar across temperatures. Power analyses confirmed high sensitivity for detecting main effects of developmental time and temperature but low power for the interaction term. Least-squares means supported these trends, showing consistent temperature-driven reductions and stage-specific shifts in metabolic rate across the dataset.

Overall, metabolic rates averaged across developmental time were assessed as a function of source and temperature (Figure 19). The analysis revealed a significant interaction between larval source and temperature, indicating that the metabolic response to temperature differed between field- and nursery-derived larvae. Although temperature alone did not significantly affect oxygen-consumption rates, the interaction ($P = 0.043$) shows that the effect of temperature depends on larval origin. Field larvae exhibited higher metabolic rates overall, and this difference was especially pronounced at 30°C, where field larvae had more than double the metabolic rate of nursery larvae (0.0559 vs. 0.0217 nmol O_2/min/larva). At 26°C, however, the two sources did not differ significantly.

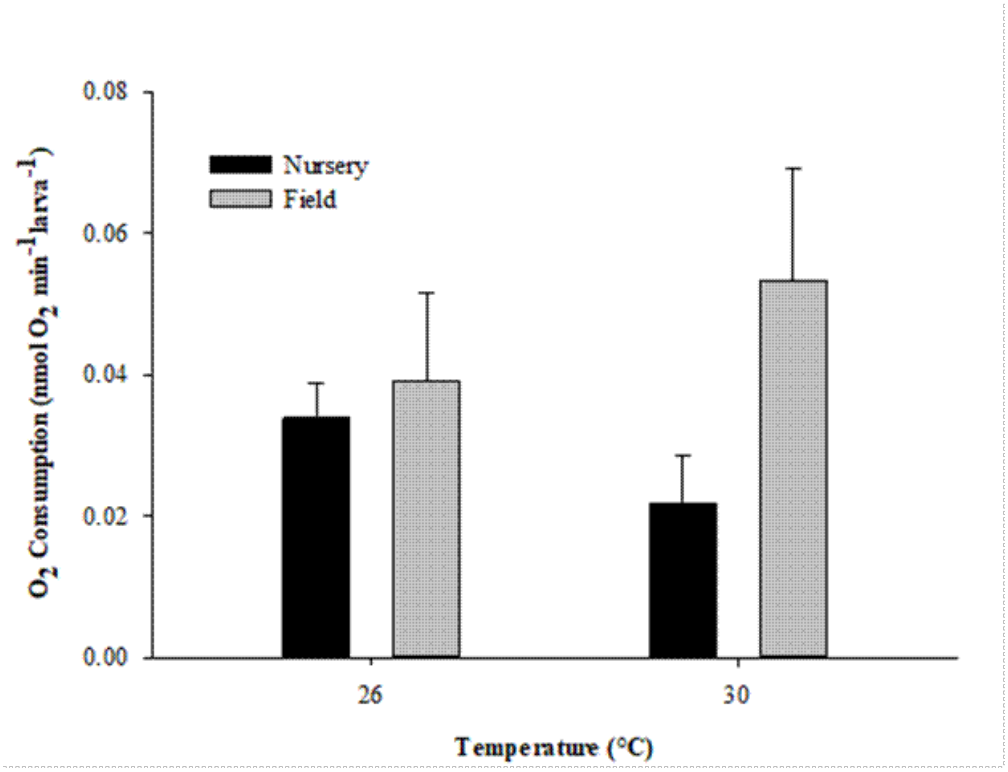

Fig 19. Summary of aerobic metabolism of *D. labyrinthiformis* larva form field collected gametes and from nursery collected gametes. Each bar represents the average measure across development (20.5-73.5hrs post fertilization). Mean ±SEM are shown (n=27).

- Metabolic response of nursery *D. labyrinthiformis* larvae to glucose

Across treatments, oxygen-consumption rates were consistently higher at 30°C than at 26°C, and glucose addition elevated metabolic rates relative to filtered seawater alone (Figure 20). In filtered seawater, mean metabolic rate increased from 0.0233 at 26°C to 0.0399 O2 min-1larva-1 at 30°C, with similar standard errors (0.00408–0.0061). A comparable pattern was observed in the glucose-enriched treatment, where metabolic rates rose from 0.0334 O2 min-1larva-1 at 26°C to 0.0464 O2 min-1larva-1 at 30°C. Variability was modest across all groups (SD ≈ 0.008–0.012), and confidence intervals overlapped slightly but remained narrow, indicating reasonably consistent measurements within each treatment–temperature combination. Overall, both warming and glucose supplementation were associated with higher mean metabolic rates, with the strongest values observed in glucose-treated larvae at 30°C.

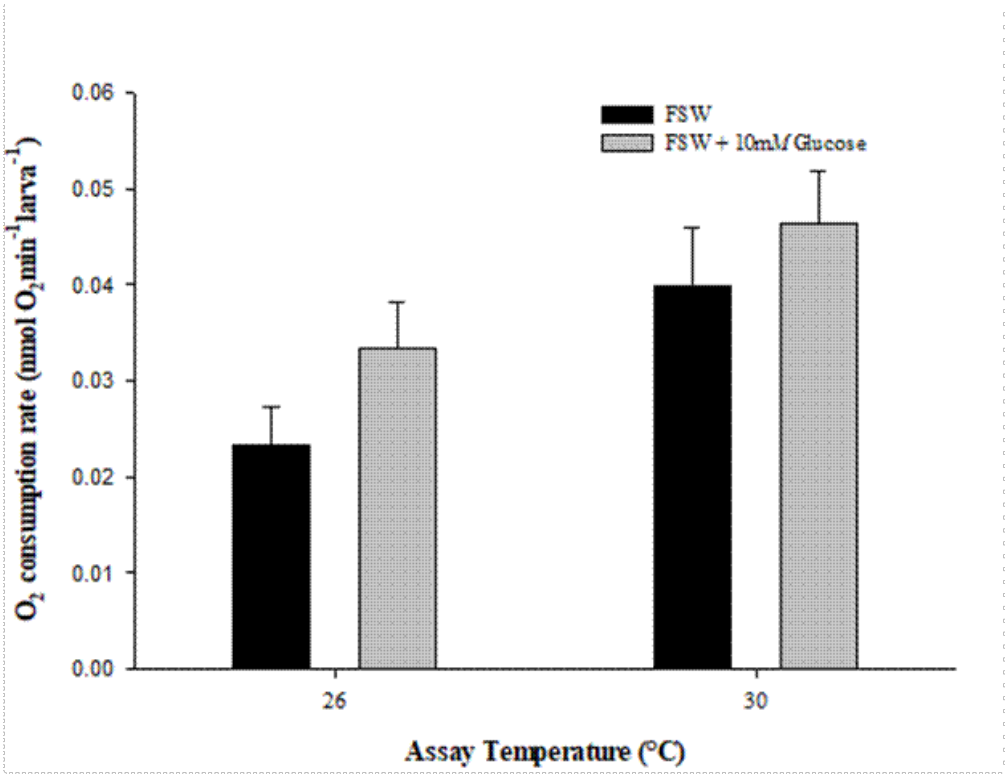

Fig 20. Aerobic metabolism of *D. labyrinthiformis* from nursery collected gametes after 72hr exposure to 0.20µm filtered seawater (FSW) and FSW containing 10m*M* glucose. Each bar represents the average measure across development (20.5-73.5hrs post fertilization). Mean ±SEM are shown (n=27).

The two-way ANOVA revealed that temperature had a significant effect on glucose-specific metabolic rate ($F_{1,14} = 8.08$, $P = 0.013$), with larvae at 30°C exhibiting higher metabolic rates (LS mean = 0.0431 ± 0.0037) than those at 26°C (LS mean = 0.0283 ± 0.0037). Holm–Sidak pairwise comparisons confirmed this temperature difference as statistically significant. In contrast, treatment (FSW vs. FSW+Glu) did not significantly influence metabolic rate ($F_{1,14} = 2.55$, $P = 0.133$), and no interaction between treatment and temperature was detected ($F_{1,14} = 0.12$, $P = 0.731$), indicating that the metabolic response to temperature was consistent across treatments. Power analyses suggested adequate power for detecting temperature effects (0.702) but low power for the glucose treatment and interaction terms. Together, these results demonstrate that

temperature, but not glucose treatment, is the primary driver of variation in glucose metabolic rate under the conditions tested.

- Enzyme activity

Across enzymes, field larvae generally exhibited higher anaerobic enzyme activities (LDH, ADH, SDH), whereas nursery larvae showed a strong late-stage increase in aerobic capacity (CS). These contrasting patterns suggest that larvae originating from different gamete sources may rely on distinct metabolic strategies during early development, with nursery larvae shifting toward enhanced aerobic metabolism as development progresses.

Anaerobic dehydrogenases

LDH activity exhibited a significant effect of gamete source ($P = 0.027$), with field-origin larvae showing higher activity than nursery larvae, while developmental time had no significant main effect ($P = 0.148$). The interaction between developmental time and source was not significant ($P = 0.073$). Post hoc comparisons indicated that source differences were present only in early larvae, and developmental differences were present only within field larvae. ADH activity showed a similar pattern: a significant source effect ($P = 0.019$), no developmental effect ($P = 0.187$), and no interaction ($P = 0.126$). Field larvae again exhibited higher activity than nursery larvae, with the largest difference occurring in early development. For both LDH and ADH, statistical power was moderate for detecting source effects but low for developmental and interaction effects.

In contrast, SDH activity did not differ significantly with respect to developmental time ($P = 0.732$), source ($P = 0.061$), or their interaction ($P = 0.603$). Although mean activity tended to be higher in field larvae, these differences were not statistically supported, and power was low across all factors. Together, the three anaerobic dehydrogenases indicate that field larvae generally exhibit higher anaerobic metabolic capacity, but the strength and consistency of this pattern vary among enzymes.

Aerobic metabolism

CS activity displayed a markedly different pattern, with a strong and statistically significant interaction between developmental time and gamete source ($P < 0.001$; Figure 21). This interaction reflected divergent developmental trajectories: field larvae showed slightly higher CS activity in early development that declined over time, whereas nursery larvae exhibited a pronounced increase in CS activity from early to late development. Post hoc comparisons confirmed that source differences were absent in early larvae but highly significant in late larvae ($P < 0.001$), and developmental differences were significant only within nursery larvae ($P < 0.001$). Statistical power was high for all CS effects, particularly the interaction.

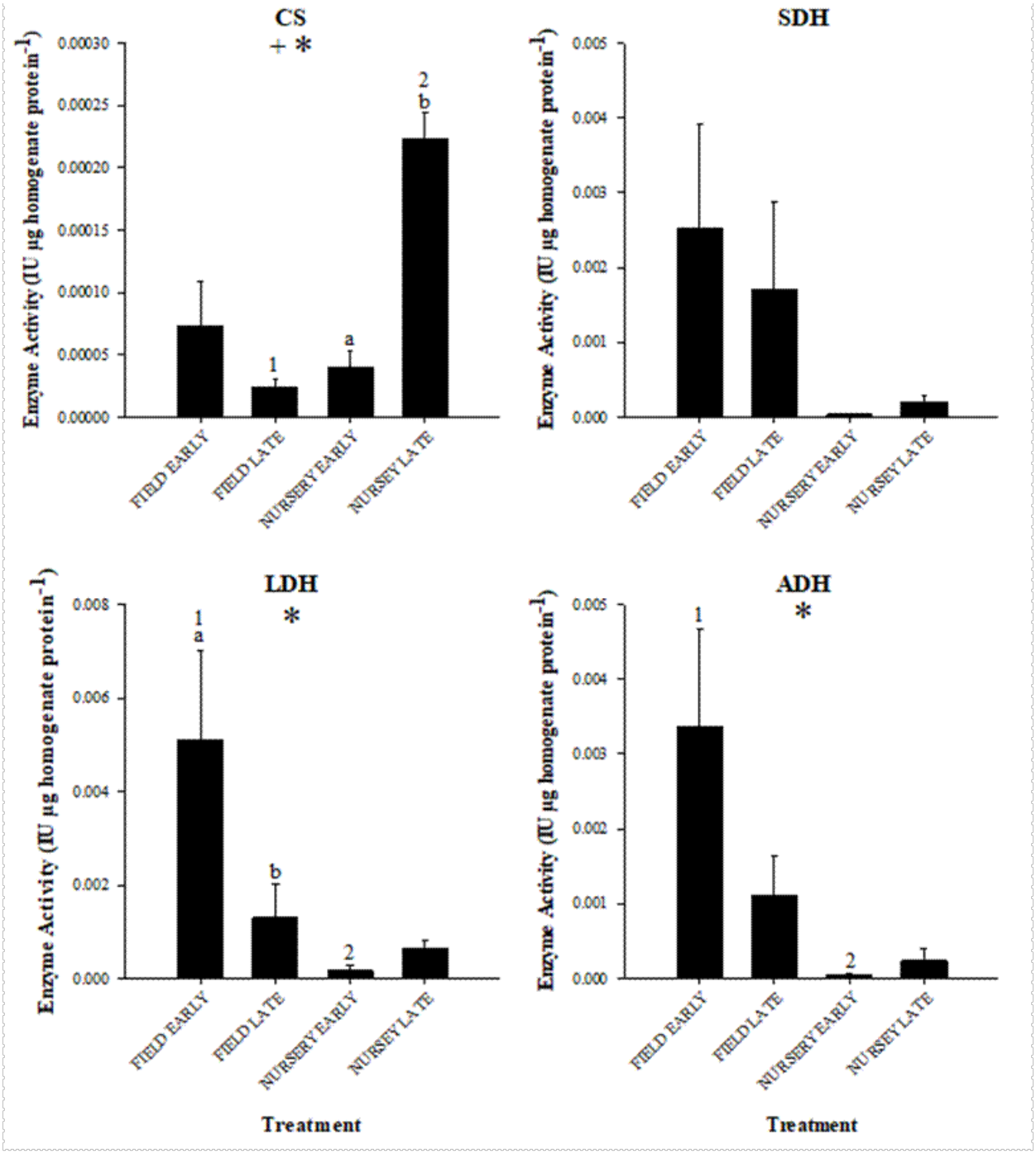

Fig 21: Enzyme activity of *D. labyrinthiformis* larvae as a function of gamete source and developmental time. Each panel presents activity for one enzyme, with comparisons between larvae originating from field-spawned versus nursery-spawned gametes at early and late developmental stages. Lowercase letters (a,b) denote significant differences within gamete origin groups (e.g., early vs. late within field). Numbers (1,2) denote significant differences within

developmental stages (e.g., field vs. nursery within late). Asterisks (*) indicate significant differences between origin groups overall (field vs. nursery), and plus signs (+) indicate significant differences between developmental stages overall (early vs. late). Error bars represent standard errors of the means.

- Statistical output

LDH

Lactate dehydrogenase (LDH) activity met assumptions of normality (Shapiro–Wilk, P = 0.094) and homogeneity of variance (P = 0.080). A two-way ANOVA testing the effects of developmental time (early vs. late) and source of gametes (field vs. nursery) revealed no significant main effect of developmental time on LDH activity ($F_{1,8} = 2.561$, P = 0.148). In contrast, LDH activity differed significantly between gamete sources ($F_{1,8} = 7.302$, P = 0.027), with field-derived larvae exhibiting higher activity than nursery-derived larvae (Figure 21). The interaction between developmental time and source was not statistically significant ($F_{1,8} = 4.254$, P = 0.073), indicating that the effect of developmental time did not depend on gamete origin.

Post hoc comparisons supported these patterns. Within the early developmental stage, LDH activity was significantly higher in field larvae than in nursery larvae (P = 0.010), whereas no difference between sources was detected in late larvae (P = 0.663). Within field-origin larvae, early individuals exhibited higher LDH activity than late individuals (P = 0.032), but developmental time had no effect within nursery larvae (P = 0.752). Least-square means for the treatment-by-source combinations further reflected these trends, with the highest activity observed in early field larvae and the lowest in early nursery larvae (Figure 21).

ADH

Alanopine dehydrogenase (ADH) activity satisfied assumptions of normality (Shapiro–Wilk, P = 0.133) and homogeneity of variance (P = 0.105). A two-way ANOVA testing the effects of developmental time (early vs. late) and gamete source (field vs. nursery) indicated no significant main effect of developmental time on ADH activity ($F_{1,8} = 2.081$, P = 0.187). In contrast, ADH activity differed significantly between gamete sources ($F_{1,8} = 8.585$, P = 0.019), with field-origin larvae exhibiting higher activity than nursery-origin larvae. The interaction between

developmental time and source was not statistically significant ($F_{1,8} = 2.920$, $P = 0.126$), indicating that the effect of developmental time did not depend on gamete origin.

Post hoc comparisons confirmed a significant difference between field and nursery larvae overall ($P = 0.019$). Least-square means for the treatment-by-source combinations showed the highest ADH activity in early field larvae and the lowest in early nursery larvae, consistent with the strong source effect (Figure 21). Developmental time differences within each source were not statistically significant.

SDH

Strombine dehydrogenase (SDH) activity met assumptions of homogeneity of variance ($P = 0.426$). A two-way ANOVA evaluating the effects of developmental time (early vs. late) and gamete source (field vs. nursery) detected no significant main effect of developmental time on SDH activity ($F_{1,8} = 0.126$, $P = 0.732$). Similarly, the main effect of gamete source was not statistically significant ($F_{1,8} = 4.737$, $P = 0.061$), although field larvae exhibited higher mean activity than nursery larvae. The interaction between developmental time and source was also non-significant ($F_{1,8} = 0.294$, $P = 0.603$), indicating that developmental stage did not modify the effect of gamete origin on SDH activity.

Means for the treatment-by-source combinations showed the highest SDH activity in early field larvae and the lowest in early nursery larvae, but these differences were not statistically supported. Overall, SDH activity exhibited substantial variability relative to effect size, and statistical power was low for all factors (treatment: 0.050; source: 0.390; interaction: 0.050), limiting the ability to detect small or moderate differences.

CS

Citrate synthase (CS) activity met assumptions of normality (Shapiro–Wilk, $P = 0.421$) and homogeneity of variance ($P = 0.578$). A two-way ANOVA revealed a significant interaction between developmental time (early vs. late) and gamete source (field vs. nursery) ($F_{1,8} = 27.517$, $P < 0.001$), indicating that the effect of developmental time on CS activity differed depending on gamete origin. Because of this interaction, main effects cannot be interpreted independently.

Least-square means demonstrated contrasting patterns between sources. In field-origin larvae, CS activity was slightly higher in early individuals than in late individuals (0.0000241 IU), although

this difference was not statistically significant (P = 0.156; Figure 21). In nursery-origin larvae, however, CS activity increased sharply from early to late development, and this difference was statistically significant (P < 0.001). Comparisons within developmental stages further supported this pattern: field and nursery larvae did not differ in early development (P = 0.329), but nursery larvae exhibited substantially higher CS activity than field larvae in late development (P < 0.001). Overall, the interaction reflected a divergence in metabolic trajectories between sources, with nursery larvae showing a pronounced increase in CS activity over time, while field larvae showed a slight decline. Statistical power was high for detecting effects of treatment (0.713), source (0.900), and especially the interaction (0.996), indicating strong sensitivity to the observed differences**.**

- **CONCLUSION & RECOMMENDATIONS**
    - **Task 2: Coral spawning and gamete collection at land-based nursery (Figueiredo)**

The species where there was no spawning observed (*P. clivosa, P. strigosa, C. natans,* and *O. faveolata*) had an extended cycle to adjust to the Tri-ACSC. This extension likely caused gamete reabsorption, which was an outcome we considered highly possible. For the next year, the corals will have been in the induction system for a full 12 month cycle with the correct environmental cues, and as such, we expect that spawning will occur next year.

Additional lights are going to be added to the tanks for more uniform lighting across the raceways. This will also help with the environmental cues necessary to induce spawning.

- **Task 3: Fertilization, larval culture and settlement (Figueiredo)**

Montastraea cavernosa larvae settled on four tiles following the 2025 spawning season. Due to the low settlement numbers, there were no survivors following three months after this spawning season.

Diploria labyrinthiformis in the induction system only released dribbles from four different colonies. One colony that dribbled was not releasing complete bundles. That colony was temporarily brought in from the field as a coral of opportunity, and likely experienced bleaching in the summer of 2025, which could have impacted gametogenesis. Although the gametes collected from the field and the induction system had high fertilization rates, the *D. labyrinthiformis* larvae did not settle well. This could have been due to low amounts of CCA on the tiles or the larvae not liking the CCA species that was used on the tiles. The lab is testing the CCA and is working on receiving good settlement inducing CCA from another facility with the goal of culturing it for future use. Most of the larvae that settled were found on the bottom of the tiles. Several tiles had skeletons, which could be an indicator of an anoxic environment in the baskets. A new aeration system is being developed to mitigate this issue in the future.

All conical tanks in the lab were updated with Hartford Loops in March 2026, to prevent larvae from getting stuck on any protrusions at the water's surface and thus expected to increase larval survival and reduce labor. The upgraded systems worked well with the larvae that were produced in May, but there was some clumping around the sides of the conical tanks. A new spray bar system is being developed to create water movement along the sides of the tank to reduce clumping.

- **Task 4: Grow-out of the newly settled corals in the land-based nursery (Figueiredo)**

A mortality event occurred in the indoor raceways on November 3rd, 2025. Surviving corals were moved to the outdoor tanks. Triton tests were sent out; however, nothing came back abnormal. We believe the light system may have been faulty, and excessive light killed the newly settled corals. Timers were purchased and installed to automatically reset the systems, to mitigate any issues in the future. Nest cameras were also purchased to monitor the tanks and lights. Three stage filters have also been purchased for the grow-out systems in lab 242 for an extra layer of protection against contaminants in the water. The filters will be installed in the upcoming months.

Juveniles that were moved to the outdoor nursery three months post-settlement did well. Hydrogen peroxide was brushed onto the plugs to kill any algae growing, which reduced competition for the juveniles as they grew. This method was successful and will be continued with future juveniles.

- **Task 5: Preserve coral genotypes of disease impacted species and induce gonad maturation and spawning in captivity (Figueiredo)**

Adult colonies were maintained well throughout the year. In the past, *M. cavernosa* and *P. strigosa* colonies had mortality events post-spawning. In December 2025, PAR levels were raised during their programmed winter months with the hopes that it will increase energy and speed up recovery after spawning.

Some health issues arose towards the bottom of the colonies, signaling that there might not be enough water flowing lower in the raceways. Additional pumps have been purchased to increase water movement at the bottom of the tanks.

Water quality was held steady throughout the year, and colonies were healthy overall. There were 41 colonies that showed health problems. Of those colonies, 22 have recovered, 8 are currently sick, and 11 have died. Sick colonies will continue to be treated and monitored. Similar to the juveniles, hydrogen peroxide has been used on adult colonies to reduce algal growth.

- **Task 6: Grow-out of coral juveniles at the offshore nursery (Gilliam)**

Predation is still a challenge at both nursery and outplant sites for juvenile corals. Species and size appear to be major drivers of predation pressure. Small corals (<2cm) don't do well due to a combination of predation and overgrowth competition. The PEDs are effective at reducing predation but require a lot of maintenance and effort to make and deploy. The offshore nursery acclimation and grow out stage appears critical to increase coral size prior to outplanting. Direct

outplanting can be effective at certain sites and with specific species, but corals need to be at least 3cm to maximize survival.

- **Task 7: Settlement trials with CYPRO (Figueiredo & Schupp)**

CYPRO functions as an inducing settlement cue for *D. labyrinthiformis* larvae, however in moderate success rates. However, compared to commonly used settlement inducers such as CCA or mature biofilms, CYPRO is bacterial producible, controllable and storable, and independent from environmental factors. The PRIMING experiment indicated potential for upscaling. In future experiments, large-scale CYPRO application methods should be developed to use it for restoration purposes. Furthermore, it would be interesting to combine settlement cues, such as biofilm, CCA, and CYPRO to test if this would increase settlement rates.

- **Task 8: Genome-wide parentage analysis and thermal stress response of parental colonies (Gomez-Corrales and Liberman)**

The temperature characterization establishes that CBASS-1 and CBASS-2 delivered their assigned thermal doses with deviations of less than 0.3°C from target, and that the Control held stable at 26.08°C ±0.13°C throughout. The Control tank's stability is essential for data interpretation: it confirms that any Fv/Fm decline observed in Control colonies reflected tank-transfer and handling stress rather than inadvertent thermal exposure. This shared handling-stress baseline, applied equally across treatments, was the most likely explanation for the absence of a statistically significant group-level treatment difference ($p = 0.668$) and underscores the importance of acclimation periods in future CBASS runs at this facility.

The equivalent overnight temperatures across all three tanks (25.97–26.18°C; Table 6) confirm that differences in Fv/Fm at the May 13 recovery measurement are attributable to thermal history during the preceding 24 hours, not to ongoing temperature differences at the time of measurement. Taken together, the temperature and Fv/Fm data support a dose-dependent thermal effect: the +6°C treatment (32.29°C for 3 hours) produced a significant group-level decline ($p = 0.006$, Tukey-

adjusted) and significant declines in all three individual colonies in that treatment. The +3°C treatment (29.05°C for 3 hours) produced declines in all three treated colonies at the individual level yet lacked the group-level statistical power ($n = 3$) to reach significance — a limitation of sample size, not necessarily evidence of a weaker biological effect.

The differential recovery trajectories observed after returning to equivalent ambient temperatures are the most directly actionable findings for restoration planning. Colony 7 (+6°C) remained significantly depressed at recovery ($p = 0.007$) while Colonies 2 and 3 had largely restored baseline Fv/Fm within 24 hours; Colony 1 (+3°C) continued to decline rather than recover ($p < 0.001$). These responses — observed under identical post-heat conditions — represent preliminary evidence of genotype-level differences in thermal resilience within this SCTLD-survivor cohort from the KJCAP. Once WGS parentage assignments are completed (Ongoing Analyses), it will be possible to test directly whether colonies with stronger recovery capacity share common broodstock parents, establishing a genetic basis for thermal tolerance that can guide future broodstock curation and outplant prioritization under DEP's Phase VII restoration targets.

This pilot experiment establishes that the CBASS system at NSU delivers reproducible, well-characterized thermal conditions suitable for CBASS screening, with ramp, hold, and cool-down profiles now validated as calibration references for future experimental sessions (Table 6; Figures 12-14). Scaling to $n \geq 6–8$ colonies per treatment, extending pre-experiment acclimation to reduce handling stress, and expanding the baseline monitoring period would substantially increase statistical power. These improvements, combined with ongoing WGS-based parentage and symbiont analyses, will position the project to deliver quantitative thermal-tolerance rankings for the KJCAP broodstock cohort by the end of Year 2.

- Symbiont associations of broodstock and nursery-reared juveniles.

Algal symbiont genotyping based on the chloroplast 23S ribosomal RNA gene (cp23S; Figure 17) revealed a clear difference in symbiont association between the two generations held at the NSU land-based nursery. The broodstock colonines were almost exclusively associated with

Cladocopium (clade C), the symbiont genus most commonly reported from *M. cavernosa* on Florida's Coral Reef (Serrano et al. 2014). Only one broodstock colony (MC24_02) hosted *Durusdinium* (clade D). In contrast, all nine juveniles produced from the 2024 spawning season and reared at the nursery hosted *Durusdinium*. Because broadcast-spawning corals such as *M. cavernosa* typically acquire their symbionts from the surrounding environment rather than inheriting them directly from the parental colonies (Baird et al. 2009), this difference most likely reflects which symbionts were available and successfully established under nursery rearing conditions.

Durusdinium is generally associated with greater thermal tolerance than *Cladocopium*, and its dominance in the juvenile cohort is therefore a potentially favorable trait for outplants destined for sites that experience periodic heat stress. At the same time, this pattern may also indicate that nursery rearing conditions favor *Durusdinium* uptake over the *Cladocopium*-dominant associations seen on the natural reef. Understanding which of these dynamics is at play has direct implications for nursery husbandry and for predicting how nursery-reared juveniles will perform once outplanted and is therefore an important target for follow-up work. The shared *Durusdinium* association across all nine CBASS juveniles also helps interpret the colony-level variation in thermal recovery observed in the CBASS experiment: because the symbiont genus was the same in all juveniles, the differences in recovery trajectory among individual colonies are more plausibly attributable to coral host genotype than to differences in symbiont identity.

The cp23S Sanger sequencing approach used here identifies only the most abundant (dominant) symbiont in each colony and does not detect background or low-abundance symbiont types that may also be present. This is an important consideration for the juvenile cohort in particular: coral recruits commonly host mixed symbiont communities containing multiple genera during early development, with the dominant symbiont shifting as the juvenile matures and the community is progressively narrowed — a process known as "winnowing" that can take several years to reach the stable assemblage characteristic of adult colonies (Poland and Cofroth 2017; Liberman et al. 2024). It is therefore likely that the broodstock and especially the juvenile symbiont communities are more diverse than the current Sanger-based results suggest, and that some individuals host mixed *Cladocopium–Durusdinium* communities not visible at this level of resolution. The higher-

resolution ITS2 metabarcoding planned for Year 2 will reveal the full symbiont community in each colony, including low-abundance background members, and will determine whether finer-scale differences in symbiont community composition contribute to the variation in thermal performance observed in the CBASS experiment. Combined with the whole-genome sequencing-based parentage assignments (Ongoing Analyses), this information will support broodstock and outplant selection decisions aimed at maximizing thermal resilience in restored *M. cavernosa* populations within the Kristen Jacobs Coral Aquatic Preserve.

- Ongoing Analyses

All 22 samples — 13 broodstock DNA extracts (Table 5) and 9 CBASS juvenile extracts (Table 7) — have been submitted to the University of Florida ICBR Gene Expression and Genotyping Core for library preparation and whole-genome sequencing on an Illumina NovaSeq X (10B, 2×150 bp; ~375 Gb output). Libraries were prepared in June 2026, and sequencing is expected in July 2026. Following data delivery, SNP calling will be performed using ANGSD, providing genotypic data for parentage analysis (COLONY/SEQUOIA) and estimation of effective population size (NeEstimator) (Hernández-Agreda et al., 2024). These analyses will clarify the reproductive contributions of individual broodstock genotypes to the juvenile cohort, and — combined with CBASS Fv/Fm responses — will enable assessment of whether parental genotype predicts offspring thermal resilience.

- **Task 9: Assessing energetics of coral early life stages and breeding stock to enhance nursery efficiencies (Martinez)**

- Metabolism

The temperature dependence of aerobic metabolism diverged between field- and nursery-derived larvae only at 30°C, indicating that the two sources express distinct thermal performance curves (TPCs). Field larvae showed their highest oxygen-consumption rates at 30°C, with aerobic metabolic output increasing consistently across developmental time. In contrast, nursery larvae exhibited their highest metabolism closer to 26°C, with a marked depression in oxygen

consumption at 30°C, particularly at mid-development. This mismatch in thermal optima suggests that the two larval sources do not share a common metabolic response to warming, despite being reared under identical hatchery conditions.

Because all larvae were hatched and assayed in a common environment, the observed differences are unlikely to reflect acute acclimation and instead point toward carryover effects from parental thermal history. Field-collected adults experience broader and more variable thermal regimes, including frequent exposure to temperatures near 30°C, which may shift offspring TPCs toward higher optima. Nursery broodstock, by contrast, are maintained under more stable and typically cooler conditions, potentially biasing larval metabolic phenotypes toward lower thermal optima. Together, these patterns are consistent with parental environmental effects or transgenerational plasticity, where the thermal environment experienced by adults shapes the metabolic performance landscape of their offspring.

- Enzyme activity

Patterns in metabolic enzyme activity revealed that larval physiology differed markedly between field- and nursery-origin gametes, suggesting that parental environment plays a central role in shaping early metabolic phenotype. Field-origin larvae consistently exhibited higher activities of anaerobic dehydrogenases (LDH, ADH, SDH), indicating greater reliance on anaerobic pathways during early development. This pattern aligns with the metabolic framework described for *Favia gravida* larvae by Pereira et al. (2020), who observed that LDH activity increased under moderate salinity stress while CS remained stable, while suggesting that stress may increase in anaerobiosis potential to repair damage and compensate for additional physiological and biochemical activity. The elevated anaerobic capacity in field larvae may therefore reflect parental exposure to more variable or stressful environmental conditions, resulting in offspring with enhanced metabolic flexibility.

In contrast, nursery larvae exhibited markedly lower anaerobic enzyme activities but showed a dramatic late-stage increase in citrate synthase (CS), indicating enhanced aerobic capacity. Pereira

et al. (2020) reported that CS activity remained unaltered for all treatments, suggesting that aerobic metabolism is relatively stable under acute environmental stress. The strong interaction observed in our dataset, where CS increased sharply only in nursery larvae, suggests that aerobic capacity is more sensitive to parental conditioning and developmental programming than to short-term environmental exposure. This divergence implies that nursery larvae may rely more heavily in aerobic pathways as development progresses, potentially reflecting reduced early stress and greater energetic resources available for mitochondrial maturation.

Together, these results suggest that larvae from different gamete sources adopt distinct metabolic strategies. Field larvae appear to maintain a stress-tolerant, anaerobically-biased phenotype, consistent with the elevated LDH responses observed under stress in Pereira et al. (2020). Nursery larvae, by contrast, develop a more aerobic phenotype later in ontogeny, potentially enhancing growth and settlement potential under stable conditions. These contrasting trajectories highlight the importance of parental environment in shaping larval metabolic performance and may have implications for coral restoration, where broodstock conditioning and nursery practices influence larval quality, resilience, and recruitment success.

- Recommendations

Match larval rearing conditions to broodstock origin.

Field-derived larvae consistently perform better at warmer temperatures (~30 °C), supported by their higher anaerobic enzyme activity (LDH, ADH, SDH), which reflects a stress-tolerant, high-demand metabolic phenotype. Nursery-derived larvae, by contrast, maintain greater metabolic stability at ~26 °C and show vulnerability to thermal stress during mid-development. Management application:

- Use 30 °C only when working with field-origin larvae, especially during early development when anaerobic capacity is highest.
- Maintain 26 °C for nursery-origin larvae to avoid metabolic depression and ensure stable development.

- When broodstock origin is mixed or unknown, default to 26 °C to minimize risk. This temperature-matching strategy reduces metabolic stress, improves larval survival, and increases the likelihood of successful settlement.

Incorporate broodstock environmental history into routine management.

Larval metabolic differences persisted despite identical rearing conditions, demonstrating strong parental carryover effects. Broodstock exposed to variable temperatures, flow, and natural foraging conditions produce larvae with more robust anaerobic capacity.

Management application:

- Maintain broodstock logs that track temperature, flow regime, feeding schedule, and spawning history.
- Use broodstock conditioning (e.g., mild thermal variability, naturalistic feeding) to enhance larval metabolic resilience.
- Prioritize broodstock with known environmental histories for high-value restoration cohorts. This improves predictability of larval performance and allows managers to intentionally shape larval metabolic phenotypes.

Optimize developmental staging and environmental control.

Early (20–25 hpf) and mid-development (40–50 hpf) are critical metabolic transition points. Nursery-origin larvae show a pronounced metabolic depression at 30 °C during mid-development, while field larvae remain stable.

Management application:

- Avoid exposing nursery larvae to 30 °C between 40–50 hpf, when they are most vulnerable.
- Introduce mild, controlled variability in temperature, flow, and light to mimic natural conditions and promote balanced anaerobic–aerobic development.
- Schedule metabolic checks or developmental assessments at these key time points. This reduces developmental bottlenecks and improves larval robustness during sensitive windows.

Support metabolic transitions with targeted husbandry.

Nursery larvae exhibit a strong late-stage increase in citrate synthase (CS), indicating rising aerobic demand and mitochondrial activity.

Management application:

- Increase aeration and water movement during late development to support oxygen-intensive aerobic metabolism.
- Adjust feeding regimes to include higher-quality or energy-dense diets that support mitochondrial ATP production. Consider exploring the supplemental feeding of lipid-rich and amino acid-rich lipid preparations.
- Consider supplemental energy sources (see previous bullet) during thermal stress or when larvae show signs of metabolic suppression. These interventions help larvae meet rising energetic demands and improve settlement readiness.

- **REFERENCES**

Agostini et al. 2013. Respiratory electron transport system activity in symbiotic corals and its link to calcification. Aquatic Biology, 18(2):125-139.

Agostini et al. 2021. Greater mitochondrial energy production provides resistance to ocean acidification in “winning” hermatypic corals. Frontiers in Marine Science 7: 600836.

Craggs et al. 2017. Inducing broadcast coral spawning ex situ: closed system mesocosm design and husbandry protocol. Ecology and Evolution 7:11066-11078.

Eigentler et al. 2012. Selected media and chemicals for respirometry with mitochondria and permeabilized cells. Mitochondrial Physiol Netw, 3:1-9.

Evensen, N. R., Parker, K. E., Oliver, T. A., Palumbi, S. R., Logan, C. A., Ryan, J. S., Klepac, C. N., Perna, G., Warner, M. E., & Voolstra, C. R. (2023). The Coral Bleaching Automated Stress System (CBASS): A low-cost, portable system for standardized empirical assessments of coral thermal limits. *Limnology and Oceanography: Methods*, *21*(7), 421–434.

Fiegel et al. 2023. Detailed visualization of settlement and early development in Leptastrea purpurea reveals distinct bio-optical features. Frontiers in Marine Science 10:984656.

Fiegel, et al. 2025. Cycloprodigiosin: A multispecies settlement cue for scleractinian coral larvae. Scientific Reports 15, 27075.

Forsman et al. 2015 Growing coral larger and faster: micro-colony-fusion and a strategy for accelerating coral cover. PeerJ 3: e1313.

Gnaiger 2011. The Oxygraph for high-resolution respirometry. Mitochondrial Physiology Network, 6(1): 1-18.

Gnaiger et al. 2015. Mitochondrial coupling and capacity of oxidative phosphorylation in skeletal muscle of Inuit and Caucasians in the arctic winter. Scandinavian journal of medicine & science in sports, 25: 126-134.

Hernández-Agreda, A., Huckeba, J., Prata, K. E., Vermeij, M. J. A., & Bongaerts, P. (2024). Hybridization and inbreeding affect the survival of a critically endangered coral. *Current Biology*, S0960982224012466. https://doi.org/10.1016/j.cub.2024.09.035

Laforest et al. 2024 Induced sexual reproduction ex situ reveals bidirectional sex change of the coral Montastraea cavernosa. Coral Reefs 43:1405–1416.

Lamptey et al. 2022. Seasonal changes in mitochondrial bioenergetics and physiological performance of the bluegill sunfish, Lepomis macrochirus, from a shallow, Midwest river. Journal of Thermal Biology, 10: 103186.

Liberman, R., Voolstra, C. R., Hume, B. C. C., & Benayahu, Y. (2024). Juvenile octocorals acquire similar algal symbiont assemblages across depths. *Coral Reefs*, *43*(2), 489–496. https://doi.org/10.1007/s00338-024-02470-3

Page et al. 2018. Microfragmenting for the successful restoration of slow growing massive corals. Ecological Engineering 123: 86-94.

Pereira, C. M., Fonseca, J. S., Paiva, E. S., Costa, P. G., Mies, M., Silva, A. G., Calderon, E. N., Bianchini, A., & Castro, C. B. (2020). Larvae of the South Atlantic coral *Favia gravida* are tolerant to salinity and nutrient concentrations associated with river discharges. *Marine Environmental Research, 161*, 105118.

Petersen et al 2023. Photodegradation of a bacterial pigment and resulting hydrogen peroxide release enable coral settlement. Scientific Reports 13:3562.

Pienkowski, et al. 2024. Nature's contributions to social determinants of mental health and the role of conservation. One Earth, 7(7), 1213-1227.

Poland, D. M., & Cofroth, M. A. (2017). Trans-generational specificity within a cnidarian–algal symbiosis. *Coral Reefs*, *36*(1), 119–129.

Serrano, X., Baums, I. B., O'Reilly, K., Smith, T. B., Jones, R. J., Shearer, T. L., Nunes, F. L. D., & Baker, A. C. (2014). Geographic differences in vertical connectivity in the Caribbean coral *Montastraea cavernosa* despite high levels of horizontal connectivity at shallow depths. *Molecular Ecology*, *23*(17), 4226–4240. https://doi.org/10.1111/mec.12861

Voolstra, C. R. (2022). Empirically derived thermal thresholds of four coral species along the Red Sea using a portable and standardized experimental approach. *Coral Reefs*. https://doi.org/10.1007/s00338-022-02233-y

Walton et al. 2018. Impacts of a regional, multi-year, multi-species coral disease outbreak in Southeast Florida. Frontiers in Marine Science 5: 323.

Zhang, Z., Green, B. R., & Cavalier-Smith, T. (2000). Phylogeny of ultra-rapidly evolving dinoflagellate chloroplast genes: A possible common origin for sporozoan and dinoflagellate plastids. *Journal of Molecular Evolution*, *51*(1), 26–40. https://doi.org/10.1007/s002390010064